Technical University Dresden

Faculty of physics

Institute of nuclear and particle physics

Masterthesis

Study of anomalous gauge couplings using $W^{\pm}Z$ channel in ATLAS

Author:
Lilly Wuest

A thesis submitted in fulfillment of the requirements of the degree of

Master of Science

(M. Sc.)

First Reviewer:	Prof. Dr. Michael Kobel
Second Reviewer:	Prof. Dr. Arno Straessner
Date of submission:	6 September 2019

Selbstständigkeitserklärung

Ich versichere, dass ich die vorliegende Arbeit selbstständig verfasst und keine anderen als die angegebenen Quellen und Hilfsmittel benutzt habe. Ich reiche diese Arbeit erstmals als Prüfungsleistung ein. Mir ist bekannt, dass ein Betrugsversuch mit der Note "nicht bestanden" (5,0) geahndet wird und im Wiederholungsfall zum Ausschluss von der Erbringung weiterer Prüfungsleistungen führen kann

Dresden, September 10, 2019 Lilly Wuest

Kurzfassung

Wir untersuchten die Auswirkungen der Dimension sechs Operatoren im Rahmen der effektiven Feldtheorie der auf QCD basierenden $W^{\pm}Z$ Produktion im vollständig leptonischen Zerfallskanal $pp \rightarrow W^{\pm}Z \rightarrow \ell\nu\ell\ell$ mit bis zu zwei zusätzlichen Jets im Matrixelement und der auf EW basierenden Vektorboson Streuung $pp \rightarrow W^{\pm}Zjj \rightarrow \ell\nu\ell\ell jj$ im VBS Phasenraum auf "truth level". Der abfallende Beitrag der Dimension sechs Effekte vom inklusiven zum VBS Phasenraum wird gezeigt. Im Bereich der höchsten EFT-Empfindlichkeit $M_T^{W^{\pm}Z} > 600\,GeV$ wird der Standard Modell $W^{\pm}Z$ Wirkungsquerschnitt auf $\sigma_{SM}^{QCD} = 0.180\,fb\,(\pm 0.021\,fb\;\; stat.)$ und $\sigma_{SM}^{EW} = 0.0628\,fb\,(\pm 0.0031\,fb\;\; stat.)$ ermittelt. Der Effekt der Dimension sechs Operatoren wird unter Verwendung der neuesten ATLAS $W^{\pm}Z$ Limits auf $\sigma_{dim-6}^{QCD} = 0.0499\,fb\,(\pm 0.0031\,fb\;\; stat.)$ und $\sigma_{dim-6}^{EW} = 0.02161\,fb\,(\pm 0.00028\,fb\;\; stat.)$ bestimmt. Das entspricht einer Abweichung von $\sim 30\%$ der SM $W^{\pm}Z$ Produktion. Im VBS Phasenraum ist dies ein erheblicher Beitrag und sollte nicht, zugunsten der Dimension acht Operatoren, vernachlässigt werden.

Abstract

Kurzfassung

We studied the impact of dimension six EFTs operators of the effective field theory framework of the QCD mediated $W^{\pm}Z$ production in the fully leptonic decay channel $pp \rightarrow W^{\pm}Z \rightarrow \ell\nu\ell\ell$ with up to two additional jets in the matrix element and EW mediated Vector Boson Scattering $pp \rightarrow W^{\pm}Zjj \rightarrow \ell\nu\ell\ell jj$ in the VBS phase space on truth level. The decreasing contribution of dimension six effects from the inclusive to the VBS phase space is shown. In the range of the highest EFT sensitivity $M_T^{W^{\pm}Z} > 600\,GeV$ the Standard Model $W^{\pm}Z$ production cross section are calculated to be $\sigma_{SM}^{QCD} = 0.180\,fb\,(\pm 0.021\,fb\ \ stat.)$ and $\sigma_{SM}^{EW} = 0.0628\,fb\,(\pm 0.0031\,fb\ \ stat.)$. The dimension six EFTs operators impact is calculated using the most recent ATLAS $W^{\pm}Z$ limits to be $\sigma_{dim-6}^{QCD} = 0.0499\,fb\,(\pm 0.0031\,fb\ \ stat.)$ and $\sigma_{dim-6}^{EW} = 0.02161\,fb\,(\pm 0.00028\,fb\ \ stat.)$. Which corresponds to a deviation of $\sim 30\%$ of the SM $W^{\pm}Z$ production. In the VBS phase space this is a sizable contribution and should not be neglected in favor of dimension eight operators.

Abstract

Contents

List of Figures

List of Tables

Chapter 1

Introduction

The Standard Model of particle physics (SM) has been an extremely successful giving predictions and describing our data. Nevertheless it is also known that the SM is not able to describe all aspects of natural phenomena like gravity, dark matter, dark energy, among others. Since the SM can't be considered the ultimate theory there must be something else, new physics that we didn't detected yet. A reason that could explain why we haven't been able to observe it is that the energy scale of these phenomena is above the momentarily reachable point. This doesn't mean the new physics quest is over, if we can't directly observe new particles, we can still look for their effects via indirect searches. The idea of indirect searches is to check the known physical processes and look for unexpected deviations from them, those deviations could actually be due to impact of new physics. A manifold of effects of new physics can be described by the help of multiple theories.

Effective field theories (EFTs) have become extremely popular in the last few years. One of the reasons is that EFTs can be used in an almost model-independent way: as a extension of the SM to parametrize small deviations observed on experimental measurements of SM observables. In the EFT approach the four dimensional Lagrangian of the SM is expanded by higher dimension operators. These higher dimensional operators implementing new particle interactions. The corresponding parameters determine the extend for the impact of higher dimensional operators in the Lagrangian. This study deals with dimension six and dimension eight operators. They are responsible for anomalous triple and quadratic gauge couplings respectively.

Experimentally the anomalous triple gauge couplings are studied in diboson processes and the therefore uses the most inclusive detector phase space. On the other hand anomalous quartic gauge couplings could be studied in Vector Boson Scattering (VBS) or triboson production. The VBS process is characterized at tree level by the exchange of weak gauge bosons between two quarks or a quark and an anti-quark, which gives us direct access to both triple and quartic gauge couplings. Previous studies done at the Large Hadron Collider, provided limits on the anomalous quartic gauge couplings parameters using the VBS phase space. In the VBS phase space any deviation from the SM was attributed to dimension eight operators. In this study we want to asset the impact of dimension six EFTs operators for $W^{\pm}Z$ production in the inclusive and in the VBS phase space. We want to find out if the effects of dimension six EFTs operators in the VBS phase space can be neglected for the estimation of limits for the parameters of dimension eight operators.

Chapter 2

Theory

2.1 The Standard Model

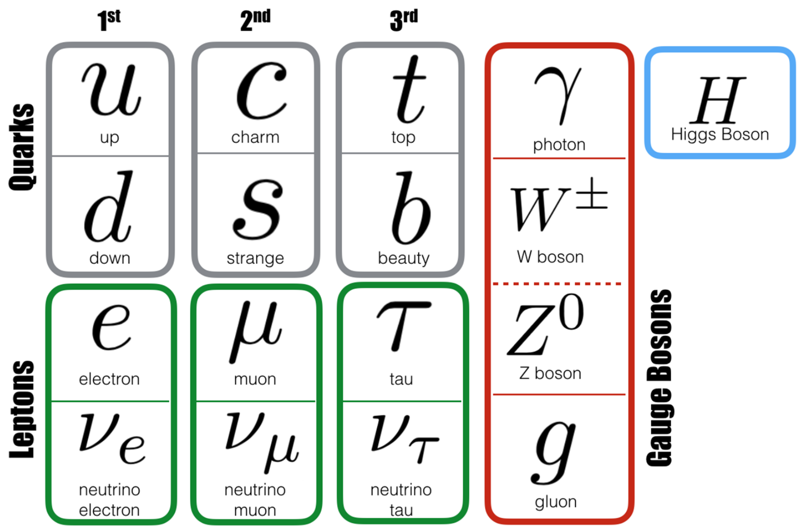

Figure 1 – The standard model particles grouped in leptons, quarks separated in flavor and the gauge bosons as well as the Higgs boson [26]

The standard model of particle physics (SM) describes the characteristics of fermions and bosons in a relativistic manner as a quantum field theory. The latter is defined through a Lagrangian $\mathcal{L}$ as its central mathematical object, while $\mathcal{L}$ is the four-dimensional density of action $S = \int d^4x\mathcal{L}\,(x)$. The Lagrangian of the standard model $\mathcal{L}_{SM}$ has a local symmetry of $U(1) \times SU(2) \times SU(3)$, is invariant under Lorentz transformations and is given by

$$\mathcal{L}_{SM} = \sum_{\psi} \bar{\psi}_L i\gamma_\mu \left(\partial^\mu + ig\frac{\sigma_a}{2}W_a^\mu + ig'\frac{Y}{2}B^\mu\right)\psi_L \tag{2.1}$$

$$+ \sum_{\psi} \bar{\psi}_R i\gamma_\mu \left(\partial^\mu + ig'\frac{Y}{2}B^\mu\right)\psi_R \tag{2.2}$$

$$- \frac{1}{4}B^{\mu\nu}B_{\mu\nu} - \frac{1}{4}W_a^{\mu\nu}W_{a\mu\nu} \tag{2.3}$$

$$+ \sum_{q} \bar{q} i\gamma_\mu \left(\partial^\mu + ig_s\frac{\lambda_a}{2}F_a^\mu\right) q - \frac{1}{4}F_{a\mu\nu}F_a^{\mu\nu} \tag{2.4}$$

$$+ \left|\left(\partial_\mu + ig\frac{\sigma_a}{2}W_a^\mu + ig'\frac{Y}{2}B^\mu\right)\Phi\right|^2 \tag{2.5}$$

$$- \left(\mu^2 |\Phi|^2 + \lambda |\Phi|^4\right) \tag{2.6}$$

with the quark field q, coupling strength g_W, g' and g_s, the Gellmann matrices λ and the gluon field F, where the index a means the three kinds of color charge, the right and left handed fermion fields $\psi_{R/L}$, the gauge fields W and B, the Pauli matrices σ_b, the weak isospin Y and the Higgs field Φ.
This is the full description of the fields and interactions of fermions and bosons. Fermions are separated in quarks and leptons and are classified in doublets of three kinds of flavours. The gauge bosons acting like intermediate particles the schematic of the SM particles is depicted in Fig. 1. The interactions between them can be distinguished into electromagnetic, strong and weak interactions.

In the SM, the electromagnetic interaction is described by the quantum electrodynamics (QED) and only acts on particles and antiparticles that carry an electric charge. The intermediate particle of QED is the photon γ which is massless. The Lagrangian of the QED $\mathcal{L}_{QED}$ remains invariant under local U(1)-transformation.

All particles of the SM are governed by the weak force. In the SM weak interactions are described by the flavour dynamics and it is the only possibility that particles may change there flavour. The local symmetry for the Lagrangian $\mathcal{L}_w$ of weak forces is given by SU(2). The weak interaction will be described together with the QED in the electroweak unification described in section 2.2.2. The Lagrangian for it will given there. The intermediate particles are of the weak interaction $W^\pm$ as charged currents and Z bosons as neutral current. They are the only intermediate particles of the SM that carry a mass ($\approx 80 - 90\,GeV$). This is the reason why weak interactions have the shortest range of all interactions.

Particles that are governed by the strong interaction carry color charge which is analog to the electric charge in the QED. Unlike the latter, not only fermions can carry a color charge but also gluons g, the massless intermediate particles of the strong force, do so. But not all fermions carry a color charge, only quarks do and are therefore the only fermions that interact strong. In the SM strong interactions are described by quantum chromodynamics (QCD) with the local symmetry group SU(3) for the Lagrangian $\mathcal{L}_{QCD}$ which is given by

$$\mathcal{L}_{QCD} = \sum_q \bar{q} i \gamma_\mu \left(\partial^\mu + i g_s \frac{\lambda_a}{2} F_a^\mu \right) q - \frac{1}{4} F_{a\mu\nu} F_a^{\mu\nu} \tag{2.7}$$

with the quark field q, the coupling strength g_s, the Gellmann matrices λ and the gluon field F, where the index a means the three kinds of color charge.

Beside the local symmetry $\mathcal{L}_{SM}$ has also global symmetries mean time reversal (T), charge conjugation (C) and parity transformation (P). The whole Lagrangian $\mathcal{L}_{SM}$ is invariant under CPT transformation (CPT theorem [12]), but parts like $\mathcal{L}_{QED}$ and $\mathcal{L}_{QCD}$ are invariant under single C and P transformations while $\mathcal{L}_{QED}$ is finally also invariant under the combined CP transformation. It is still an open question if this is also the case for $\mathcal{L}_{QCD}$. C, P and CP violations are measured for $\mathcal{L}_w$, so only CPT invariance holds true.

2.2 Electroweak Interaction

2.2.1 $W^\pm$ and Z bosons

The $W^\pm$ and Z are the massive gauge bosons of weak interactions. To produce and study them in colliders and detectors like ATLAS and CMS experiments at the Large Hadron Collider (LHC) at CERN it is necessary that the center of mass energy $\sqrt{s}$ of the colliding particles reach at least the mass of these particles. Since protons are non elementary particles the single quarks in the protons need to reach this $\sqrt{s}$. The production of $W^\pm$ and Z bosons by proton collisions is dominated by

$$u + \bar{u} \rightarrow Z \qquad d + \bar{u} \rightarrow W^- \tag{2.8}$$

$$d + \bar{d} \rightarrow Z \qquad u + \bar{d} \rightarrow W^+ \tag{2.9}$$

Since a proton consists of two up quarks u and one down quark d as valence quarks, which carry a much higher part of the total $\sqrt{s}$ as any virtual quark, the ratio of W^+ and W^- productions is not symmetric and the probability to produce a W^+ is higher than the probability to produce a W^-. The probability to produce a Z boson is higher than to producing $W^\pm$ since it can be produced with any one of the valence quarks. But Z bosons with a mass $m_Z \approx 91\,GeV$ [20] are heavier than $W^\pm$ with $m_{W^\pm} \approx 80\,GeV$ [19].
Weak gauge bosons decay by the order of $10^{-25}\,s$ [22] and don't reach any part of detector before they decay. So they need to be specified by the decay products of them. $W^\pm$ and Z bosons are able to decay hadronically and leptonically. Because of the decay in quarks and the hadronization afterwards it is more difficult to reconstruct the quark flavour of decay products. An other difficulty of hadronic decays is the amount of background products where the final state looks exactly the same. Based on the flavour color of quarks the hadronic decays happen much more often then the leptonic. But it is easier to identify $W^\pm$ and Z bosons by leptonic decays. $W^\pm$ decays leptonically in a charged lepton and a neutrino where the flavour is undecided. The neutrino is just measurable by the missing energy E_{miss} of the hole event. While the lepton can be identified by its charge and high energy. The probabilities of these decay channels are divided like

$$W^\pm \rightarrow l^\pm + \nu_l \qquad \sim 33\% \tag{2.10}$$

$$hadronic \qquad \sim 66\% \tag{2.11}$$

The interaction of $W^\pm$ is, according to the electric charge, symmetric for all flavours of fermions.
The signature of charged leptons is specially for Z really clear. One finds two leptons with opposite charge, high energy and opposite direction of flight. The possible decay channels are given by

$$Z \rightarrow l^+ + l^- \qquad \sim 10\% \tag{2.12}$$

$$\nu_l + \bar{\nu}_l \qquad \sim 20\% \tag{2.13}$$

$$hadronic \qquad \sim 70\% \tag{2.14}$$

The interaction of Z is also symmetric for all flavors but as one can see by the probability of the decays, it depends on the charge of the fermions. So there must be a different way to describe the interaction of Z bosons other than than the flavour dynamics. [22]

2.2.2 Electroweak Unification

Since the branching ratio of Z bosons depends to the electric charge of the decay particles, the kind of weak interaction should be different for these particles as for $W^{\pm}$. The characteristic of this behavior has a suitable description in the electroweak unification.

The main idea is to introduce a new quantum number, the weak isospin T. All flavors of fermions with negative helicity form a doublet of fermions which can switch into each other by absorbing or emitting a $W^{\pm}$. These doublets have an isospin of $T = 1/2$ and a third component $T_3 = \pm 1/2$. For anti-fermions with positive helicity T_3 switches its sign. Since fermions with positive and anti-fermions with negative helicity don't interact with $W^{\pm}$, this particles are singlets without a weak isospin. To make the introduction of weak isospins consistent $W^{\pm}$ also gets a value of T and T_3. By absorbing or emitting $W^{\pm}$ these gauge bosons need to have $T_3(W^+) = +1$ and $T_3(W^-) = -1$ to gain the correct T_3 for all fermions. Based on the spin formalism there is a third state of a W field W^0 with $T_3(W^0) = 0$ that doesn't change T_3 of fermions by interacting with exactly the same strength g_w like $W^{\pm}$. So we have a triplet W field of weak isospin. Due to W^0 can't be the gauge boson Z (the coupling of W^0 isn't dependence of the electric charge of particles) there have to be a further state B^0 that we postulate with $T = 0$ and $T_3 = 0$ and a different coupling strength g'. While the tree W field have the coupling strength g_W. To get the physical two gauge bosons Z and γ that doesn't change the flavour by interacting with fermions we create two orthogonal linear combinations of W^0 and B^0 and get therefore:

$$|\gamma\rangle = \cos\theta_w |B^0\rangle + \sin\theta_w |W^0\rangle \tag{2.15}$$

$$|Z\rangle = -\sin\theta_w |B^0\rangle + \cos\theta_w |W^0\rangle \tag{2.16}$$

Where θ_w is the electroweak mixing angle (also called Weinberg angle). The relation between θ_w and the coupling strength g_W, g' and the electric charge e is given by the postulation of the interaction of γ with fermions. The electroweak mixing angle is measured with $\sin^2\theta_w \approx 0.23$ [22]. The Lagrangian of the electroweak interaction results in

$$\mathcal{L}_{EW} = \sum_{\psi} \bar{\psi}_L i\gamma_\mu \left(\partial^\mu + i g_W \frac{\sigma_a}{2} W_a^\mu + i g' \frac{Y}{2} B^\mu\right) \psi_L \tag{2.17}$$

$$+ \sum_{\psi} \bar{\psi}_R i\gamma_\mu \left(\partial^\mu + i g' \frac{Y}{2} B^\mu\right) \psi_R \tag{2.18}$$

$$- \frac{1}{4} B^{\mu\nu} B_{\mu\nu} - \frac{1}{4} W_a^{\mu\nu} W_{a\mu\nu} \tag{2.19}$$

with the right and left handed fermion fields $\psi_{R/L}$, the gauge fields W and B, the coupling streght g and g', the Pauli matrices σ_b and the weak isospin Y.

2.2.3 The Higgs Mechanism

To make the list of particles in the SM complete we finally have to include the Higgs boson H. With the introduction of the electroweak unification and the $\mathcal{L}_{QCD}$ there was still an unexplained nature that was missing in the theoretical description of the standard model with $\mathcal{L}'_{SM}$ (the Lagrangian without the Higgs mechanism). The mass of the massive gauge bosons $W^{\pm}$ and Z couldn't be explained by the Lagrangian $\mathcal{L}'_{SM}$. By including of the Higgs mechanism to the $\mathcal{L}'_{SM}$ together with the electroweak unification we get by itself mass terms to this bosons. The gauge bosons γ for the electromagnetic part of the electromagnetic interaction stays massless.

$$\mathcal{L}_{Higgs} = \left| \left(\partial_\mu + ig_W \frac{\sigma_a}{2} W_b^\mu + ig' \frac{Y}{2} B^\mu \right) \Phi \right|^2 - \left(\mu^2 \left| \Phi \right|^2 + \lambda \left| \Phi \right|^4 \right) \tag{2.20}$$

with the gauge fields W and B, the coupling strength g_W and g', the Pauli matrices σ_b, the weak isospin Y and the Higgs field Φ.
The Higgs mechanism also permits mass terms for fermions by using the so called Yukawa coupling of the Higgs field to the fermion fields. As a result of the Higgs mechanism the Higgs bosons H is predicted as a resonance of the Higgs field. This measurable particle remained as the last piece of the puzzle of the SM for a long time and was finally confirmed with a mass of $m_H \approx 125\, GeV$ in 2012 by the ATLAS and CMS experiment at the LHC and showed the existence of the Higgs mechanism as a consequence [2]. More details about the Higgs mechanism [12].

2.3 Effective Field Theory

Despite the increasing center of mass energy $\sqrt{s}$ in collider experiments no direct sign of new physics has been observed yet. As a consequence the scale of new physics energy Λ must be above the currently reachable point. So it is interesting to search indirectly for the effects of new physics. One method to do so is to look for new interactions of the particles that are well know in the SM. An approach is a model independent effective quantum field theory (EFT). The main idea for the here explained EFT is to extend the four dimensional Standard Model Lagrangian $\mathcal{L}_{SM}$ (2.1) with operators of higher dimensions consistent to the known symmetry of the SM and based on a single Higgs doublet field [11]

$$\mathcal{L}_{EFT} = \mathcal{L}_{SM} + \frac{c^{(5)}}{\Lambda}\mathcal{O}^{(5)} + \sum_i \frac{c_i^{(6)}}{\Lambda^2}\mathcal{O}_i^{(6)} + \sum_j \sum_k \frac{f_j^{(6+k)}}{\Lambda^{2+k}}\mathcal{O}_j^{(6+k)} \tag{2.21}$$

where $\mathcal{O}^d$ are the operators with dimension d and c_i/Λ^{d-4} the parametrization of the energy scale in which we assume the effect of $\mathcal{O}^d$ gives a significant impact. To use this EFT as an expansion just with virtual effects and finite number of terms, the masses and momenta of the involved particles of the SM have to be significantly smaller than the energy scale Λ of the new physics. Then the terms higher order become extremely small and can be disregarded. But if the interaction energy of the particles that are responsible for new physics reaches the energy scale Λ all terms of the Lagrangian expansion become real and important [3]. So on this point the EFT will fail. For that reason (2.21) just can be used for indirect searches. Therefore we measure the tails of the new physics in the distributions of the SM particles.

For this study we are interested in the operators $\mathcal{O}^6$ and $\mathcal{O}^8$. The effects of them become apparent in the anomalous gauge couplings. In the standard model $W^\pm$ and Z are able to couple with themselves. So the SM already includes triple (TGC) and quartic (QGC) gauge couplings of the weak gauge bosons as shown in Fig. 2. Within the EFT we get additional terms of anomalous triple (aTGC) and anomalous quartic (aQGC) gauge couplings.

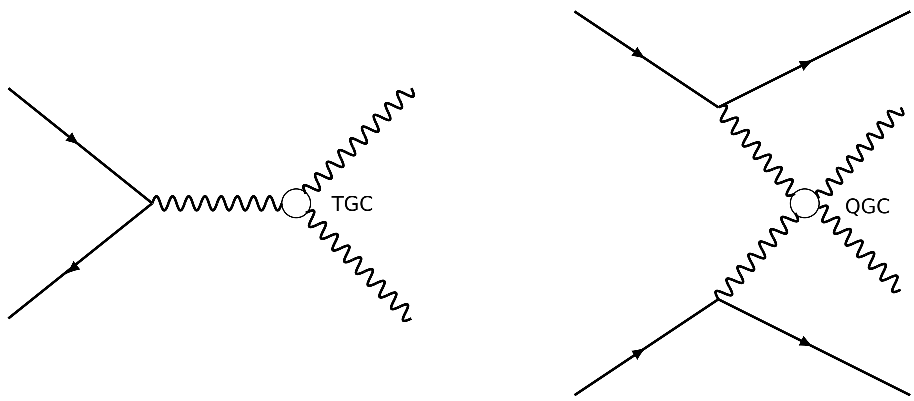

Figure 2 – Triple and quartic gauge couplings in the SM

2.3.1 Dimension six Operators $\mathcal{O}^6$

For the effect of the dimension 6 operator we use here the Warsaw basis [13]. There are additional basis for higher dimension operators. A general method to create higher dimensional bases is found in [15].

In general there are thousands of dimension six EFTs operators but only a few of them have any impact to physical processes [5]. And since we are only interested in vector boson self interaction the number of dimension six EFTs operator reduces to five. Three with conservation of C and P and two that violate CP as described in 2.1.

$$\mathcal{O}_{WWW} = Tr\left[W_{\mu\nu}W^{\nu\rho}W^{\mu}_{\rho}\right] \tag{2.22}$$
$$\mathcal{O}_{W} = (D_\mu\Phi)^\dagger W^{\mu\nu}(D_\nu\Phi) \tag{2.23}$$
$$\mathcal{O}_{B} = (D_\mu\Phi)^\dagger B^{\mu\nu}(D_\nu\Phi)\,\mathcal{O}_{\widetilde{W}WW} = \qquad Tr\left[\widetilde{W}_{\mu\nu}W^{\nu\rho}W^{\mu}_{\rho}\right] \tag{2.24}$$
$$\mathcal{O}_{\widetilde{W}} = (D_\mu\Phi)^\dagger \widetilde{W}^{\mu\nu}(D_\nu\Phi) \tag{2.25}$$

with Φ as the Higgs doublet field and

$$D_\mu = \partial_\mu + \frac{i}{2}g\tau^I W^I_\mu + \frac{i}{2}g' B_\mu \tag{2.26}$$
$$W_{\mu\nu} = \frac{i}{2}g\tau^I\left(\partial_\mu W^I_\nu - \partial_\nu W^I_\mu + g\epsilon_{IJK}W^J_\mu W^K_\nu\right) \tag{2.27}$$
$$B_{\mu\nu} = \frac{i}{2}g'\left(\partial_\mu B_\nu - \partial_\nu B_\mu\right) \tag{2.28}$$

The associated parameters c_i/Λ^2 for the dimension six EFTs operators are therefore c_{www}/Λ^2, c_w/Λ^2, c_b/Λ^2, $c_{\widetilde{W}WW}/\Lambda^2$ and $c_{\widetilde{W}}/\Lambda^2$. The limits for these parameters are already calculated for different vector boson pairs VV and also for different decay channels. The latest $W^\pm Z$ with fully leptonic decay channel depended limits of the ATLAS experiment are shown in Tab. 1. While the best limits are given for the combination of the $W^\pm W^\pm$ and $W^\pm Z$ channel with semi-leptonic decay by the CMS experiment and can be found in Tab. 2. This limits are calculated with the transverse mass of M_T^{VV} $[GeV]$ with the following binning

$$[0-140]\,,[140-180]\,,[180-250] \tag{2.29}$$
$$[250-450]\,,[450-600]\,,[600-\infty] \tag{2.30}$$

Coupling	Observed $[TeV^{-2}]$
c_w/Λ^2	$[-3.6; 7.3]$
c_{www}/Λ^2	$[-3.3; 3.2]$
c_b/Λ^2	$[-253; 136]$

Table 1 – 1D limits for dimension six parameters measured in the $W^\pm Z$ boson pair production and fully leptonic decay with ATLAS data of $\sqrt{s} = 8\,TeV$ and $\sqrt{s} = 13\,TeV$ [18].

Coupling	Observed $[TeV^{-2}]$
c_w/Λ^2	$[-2.00; 2.56]$
c_{www}/Λ^2	$[-1.58; 1.59]$
c_b/Λ^2	$[-8.78; 8.54]$

Table 2 – 1D limits for dimension six parameters measured in the $W^{\pm}Z$ and $W^{\pm}W^{\pm}$boson pair production and semi-leptonic decay with CMS data of $\sqrt{s} = 13\,TeV$ [25].

To calculate the matrix element M_{EFT} for the physical processes described by theory of the Lagrangian $\mathcal{L}_{EFT}$ the Feynman calculus is used [21]. In $\mathcal{M}_{EFT}$ we find the standard model matrix element $\mathcal{M}_{SM}$ and an additional matrix elements for the new physics induced by the further up described approach with an effective field theory $\mathcal{M}_{dim6}$. The amplitude $\mathcal{A}$ of the processes is given with $|\mathcal{A}_{EFT}|^2 \sim |\mathcal{M}_{EFT}|^2$ and therefore

$$|\mathcal{A}_{EFT}|^2 = \left|\mathcal{A}_{SM} + \sum_i \frac{c_i}{\Lambda^2}\mathcal{A}_{dim6}\right|^2 \tag{2.31}$$

$$= |\mathcal{A}_{SM}|^2 + \sum_i \frac{c_i}{\Lambda^2} 2Re\left(\mathcal{A}_{SM}^*\mathcal{A}_i\right) + \sum_i \frac{c_i^2}{\Lambda^4}|\mathcal{A}_i|^2 \tag{2.32}$$

$$+ \sum_{ij, i\neq j} \frac{c_i c_j}{\Lambda^4} 2Re\left(\mathcal{A}_i^*\mathcal{A}_j\right) \tag{2.33}$$

Where $(\mathcal{A}_{SM}^*\mathcal{A}_i)$ characterize the interference between the standard model and the beyond the standard model part. While $(\mathcal{A}_i^*\mathcal{A}_j)$ describes the cross term between different dimension six parameters c_i and c_j. So that we get a SM, an interference with the SM and the higher dimension operator, a quadratic higher dimension operator and a cross term between the different higher dimension operators.

2.3.2 Dimension eight Operators $\mathcal{O}^8$

The next operators that give an effect to the gauge or vector boson self-coupling are dimension eight operators $\mathcal{O}^8$. Here we find operators that lead to pure anomalous quartic gauge coupling. This operators can be separated in three different groups [9]. The first one just contains $D_\mu\Phi$ terms where D_μ is given by 2.26

$$\mathcal{O}_{S,0} = \left[(D_\mu\Phi)^\dagger D_\nu\Phi\right] \times \left[(D^\mu\Phi)^\dagger D^\nu\Phi\right] \tag{2.34}$$

$$\mathcal{O}_{S,1} = \left[(D_\mu\Phi)^\dagger D^\mu\Phi\right] \times \left[(D_\nu\Phi)^\dagger D^\nu\Phi\right] \tag{2.35}$$

The second type includes operators with $D_\mu\Phi$ and two field strength tensors

$$\mathcal{O}_{M,0} = Tr\left[W_{\mu\nu}W^{\mu\nu}\right] \times \left[(D_\beta\Phi)^\dagger D^\beta\Phi\right] \tag{2.36}$$
$$\mathcal{O}_{M,1} = Tr\left[W_{\mu\nu}W^{\nu\beta}\right] \times \left[(D_\beta\Phi)^\dagger D^\mu\Phi\right] \tag{2.37}$$
$$\mathcal{O}_{M,2} = \left[B_{\mu\nu}B^{\mu\nu}\right] \times \left[(D_\beta\Phi)^\dagger D^\beta\Phi\right] \tag{2.38}$$
$$\mathcal{O}_{M,3} = \left[B_{\mu\nu}B^{\nu\beta}\right] \times \left[(D_\beta\Phi)^\dagger D^\mu\Phi\right] \tag{2.39}$$
$$\mathcal{O}_{M,4} = \left[(D_\beta\Phi)^\dagger W_{\beta\nu}D^\mu\Phi\right] \times B^{\beta\nu} \tag{2.40}$$
$$\mathcal{O}_{M,5} = \left[(D_\beta\Phi)^\dagger W_{\beta\nu}D^\nu\Phi\right] \times B^{\beta\mu} \tag{2.41}$$
$$\mathcal{O}_{M,6} = \left[(D_\beta\Phi)^\dagger W_{\beta\nu}W^{\beta\nu}D^\mu\Phi\right] \tag{2.42}$$
$$\mathcal{O}_{M,7} = \left[(D_\beta\Phi)^\dagger W_{\beta\nu}W^{\beta\mu}D^\nu\Phi\right] \tag{2.43}$$

And for the last group we just find operators with field strength tensors

$$\mathcal{O}_{T,0} = Tr\left[W_{\mu\nu}W^{\mu\nu}\right] \times \left[W_{\alpha\beta}W^{\alpha\beta}\right] \tag{2.44}$$
$$\mathcal{O}_{T,1} = Tr\left[W_{\alpha\nu}W^{\mu\beta}\right] \times \left[W_{\mu\beta}W^{\alpha\nu}\right] \tag{2.45}$$
$$\mathcal{O}_{T,2} = Tr\left[W_{\alpha\mu}W^{\mu\beta}\right] \times \left[W_{\beta\nu}W^{\nu\alpha}\right] \tag{2.46}$$
$$\mathcal{O}_{T,5} = Tr\left[W_{\mu\nu}W^{\mu\nu}\right] \times B_{\alpha\beta}B^{\alpha\beta} \tag{2.47}$$
$$\mathcal{O}_{T,6} = Tr\left[W_{\alpha\nu}W^{\mu\beta}\right] \times B_{\mu\beta}B^{\alpha\nu} \tag{2.48}$$
$$\mathcal{O}_{T,7} = Tr\left[W_{\alpha\mu}W^{\mu\beta}\right] \times B_{\beta\nu}B^{\nu\alpha} \tag{2.49}$$
$$\mathcal{O}_{T,8} = B_{\mu\nu}B^{\mu\nu}B_{\alpha\beta}B^{\alpha\beta} \tag{2.50}$$
$$\mathcal{O}_{T,9} = B_{\alpha\mu}B^{\mu\beta}B_{\beta\nu}B^{\nu\alpha} \tag{2.51}$$

Where 2.34 to 2.43 including interactions of $W^\pm$, Z and γ. While additional interactions between $W\pm$ and Z are demonstrated by 2.44 - 2.49. And finally 2.50 and 2.51 describe only the self-coupling of the neutral vector boson of the electroweak interaction Z.The to the dimension eight operator $\mathcal{O}_i^8$ corresponding parameters are f_i/Λ^4. The latest 1D limits calculated by the ATLAS experiment are shown in Tab. 3

Coupling	Observed 10^3 $[TeV^{-4}]$
$f_{M,0}/\Lambda^4$	$[-0.3; 0.3]$
$f_{M,1}/\Lambda^4$	$[-0.5; 0.5]$
$f_{M,2}/\Lambda^4$	$[-1.8; 1.8]$
$f_{M,3}/\Lambda^4$	$[-3.1; 3.0]$
$f_{M,4}/\Lambda^4$	$[-1.1; 1.1]$
$f_{M,5}/\Lambda^4$	$[-1.7; 1.7]$
$f_{M,6}/\Lambda^4$	$[-0.6; 0.6]$
$f_{M,7}/\Lambda^4$	$[-1.1; 1.1]$
$f_{T,0}/\Lambda^4$	$[-0.1; 0.1]$
$f_{T,1}/\Lambda^4$	$[-0.2; 0.2]$
$f_{T,2}/\Lambda^4$	$[-0.4; 0.4]$
$f_{T,5}/\Lambda^4$	$[-1.5; 1.6]$
$f_{T,6}/\Lambda^4$	$[-1.9; 1.9]$
$f_{T,7}/\Lambda^4$	$[-4.3; 4.3]$

Table 3 – 1D limits for dimension eight parameters measured in the $W^\pm W^\pm\gamma$ and $W^\pm Z\gamma$ boson production for the semileptonic and fully leptonic decay with ATLAS data of $\sqrt{s} = 8\,TeV$ [1].

For the probability of a aQGC process we find the same separation of $|\mathcal{A}_{EFT}|^2$ as for the aTGC processes (2.31).

$$|\mathcal{A}_{EFT}|^2 = \left|\mathcal{A}_{SM} + \sum_i \frac{c_i}{\Lambda^4}\mathcal{A}_{dim8}\right|^2 \tag{2.52}$$

$$= |\mathcal{A}_{SM}|^2 + \sum_i \frac{c_i}{\Lambda^4} 2Re\left(\mathcal{A}_{SM}^*\mathcal{A}_i\right) + \sum_i \frac{c_i^2}{\Lambda^{16}}\left|\mathcal{A}_{dim8}\right|^2 \tag{2.53}$$

$$+ \sum_{ij,i\neq j} \frac{c_i c_j}{\Lambda^{16}} 2Re\left(\mathcal{A}_i^*\mathcal{A}_j\right) \tag{2.54}$$

So here also a normal quadratic SM, an interference with the SM a quadratic new physics and cross between the parameters term can be found.

2.4 Dibosons processes

To set limits to the dimension six parameters c_i/Λ^2 diboson processes are extremely appropriate. The main idea is that collisions of two protons p produce two vector bosons VV as shown in Fig. 3 and decay hadronic, semi-leptonic or completely leptonic. Whereby semi-leptonic means that one of V decays hadronic and on leptonic

$$pp \to VV \to qqqq \tag{2.55}$$
$$\to qq\ell\,(\nu)\,\ell\,(\nu) \tag{2.56}$$
$$\to \ell\ell\,(\nu)\,\ell\,(\nu) \tag{2.57}$$

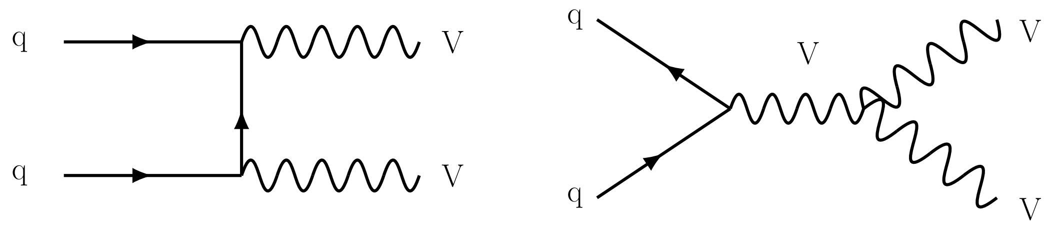

Figure 3 – Production of dibosons

On the right side of Fig. 3 we see a triple gauge boson self-coupling. Furthermore V means $W^{\pm}$, Z or could also be a Higgs bosons H. In this study we concentrate on the fully leptonic $W^{\pm}Z$ channel.

$$pp \to W^{\pm}Z \to \ell\ell\ell\nu \tag{2.58}$$

2.4.1 The inclusive phase space

Events that includes diboson processes have a special signature with which we can distinguish this events from other events that are defined as background. To reduce the background events some characteristics will be required to the particles on the events which fit to the signature of a diboson process. Since we want to study the fully leptonic decay of $W^{\pm}Z$ on truth level the inclusive phase space for it is defined as seen in Tab. 4.

Variable	inclusive phase space
$lepton\,\lvert\eta\rvert$	$<\ 2.5$
p_T of ℓ_Z , p_T of ℓ_W $[GeV]$	$> 15, > 20$
m_Z range $[GeV]$	$\left\lvert m_Z - m_Z^{PDG}\right\rvert < 10$
m_T^W $[GeV]$	> 30
$\Delta R\left(\ell_Z^{-}\ell_Z^{+}\right)$, $\Delta R\left(\ell_Z\ell_W\right)$	> 0.2, > 0.3

Table 4 – Definition of the fiducial inclusive phase space of $W^{\pm}Z$ [4]

2.5 Vector boson scattering

To set limits on the dimension eight parameters f_i/Λ^4 it is useful to have a look on Vector Boson Scattering (VBS). This means that we produce two vectors bosons VV which interact and scatter again in two vector bosons VV as shown in Fig. 2.5.1 and finally decay hadronic, semi-leptonic or leptonic. This process is only observed in the Large Hadron Collider.

$$
\begin{aligned}
pp \to VV \to VV &\to qqqq && (2.59)\\
&\to qq\ell\,(\nu)\,\ell\,(\nu) && (2.60)\\
&\to \ell\ell\ell\,(\nu)\,\ell\,(\nu) && (2.61)
\end{aligned}
$$

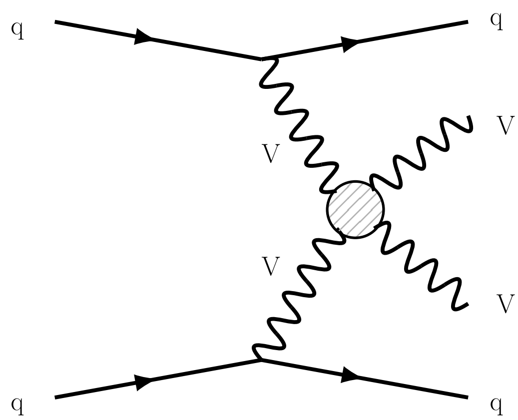

Figure 4 – Vector boson scattering (VBS)

The SM quartic gauge coupling contributes here at tree level and therefore additional dimension eight operators would give an impact to these kind of process. But there are still other opportunities as a triple gauge coupling or a Higgs interaction shown in Fig. 5. For this study we are interested in the TGC's and QGC's in VBS as explained in section 2.5.2.

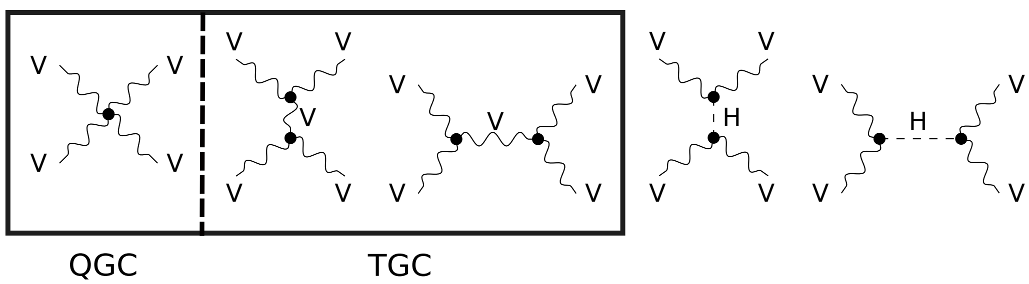

Figure 5 – Interactions by Vector Boson Scattering

Since SM quartic gauge coupling is produced in Vector Boson Scattering, anomalous quartic gauge couplings elicited by dimension eight operators changes the cross section and kinematic distributions of VBS processes.

2.5.1 The VBS phase space

The Vector Boson Scattering at the Large Hadron Collider has a special signature. If we compare the Feynman diagrams of Fig. 3 and Fig. 5 we find two vector bosons in both. But for VBS we have additional jets produced by the two quarks (Fig. /vbs). The jets associated to the VBS processes are defined as the tagging jets. Due to their origin they have some typical characteristics. Therefore the VBS phase space is defined as the inclusive phase space (shown in Tab. 4) plus some requirements to the tagging jets. Events that are passing the VBS phase space have two very energetic forward jets with a big rapidity η between them. Therefore the additional requirements for the two tagging jets are defined in Tab. 5.

Variable	VBS phase space
p_T of two leading jets $[GeV]$	> 40
$\|\eta_j\|$ of two leading jets	< 4.5
jet multiplicity	≥ 2
$\eta_{j1} \cdot \eta_{j2}$	< 0
m_{jj} $[GeV]$	> 500

Table 5 – Definition of the fiducial VBS phase space of $W^{\pm}Z$ [4]

2.5.2 Anomalous triple gauge coupling in the VBS phase space

The VBS phase space is particularly sensitive to the effects of dimension eight operators (section 2.5) and has been used in the previous ATLAS and CMS publications to extract limits. So far this is done without the consideration of dimension six EFTs operators which also have an impact on VBS signatures. Besides Vector Boson Scattering is a completely electroweak processes and has a small cross section compared to the huge amount of QCD background processes which take place in the Large Hadron Collider. Since there is a QCD mediated processes with an impact of dimension six EFTs operators (section 2.5.2) it is indispensable to study if the dimension six EFTs operators have an important

impact in the VBS phase space and thus this has to be considered by the extraction for the limits of dimension eight operators.
The processes with additional dimension six EFTs operators which can pass the VBS cuts will be described next.

QCD mediated VV production

The first category of triple gauge self-interaction in the VBS phase space is the one where the needed jets comes from strong interactions and the fully leptonic decay of the gauge bosons take place with the weak force. For the extraction of dimension six EFTs operators this is the signal process. But by having a look on Vector Boson Scattering it is the main background for electroweak VV production with the same final state. This QCD mediated process represents $\sim 70\%$ of the events selected by using the VBS phase space.

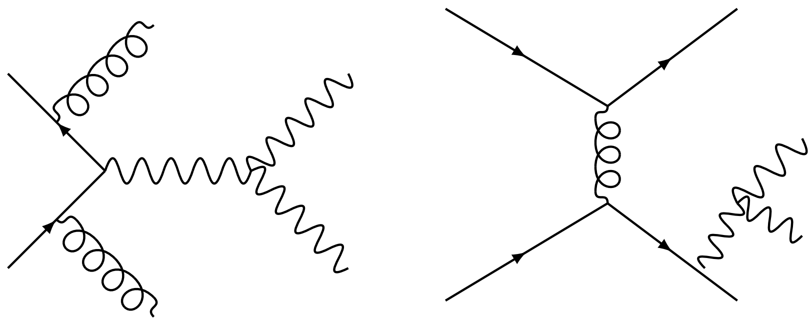

Figure 6 – Example for a QCD mediated VV production

EW mediated VV production

In the second category all vertices take place by a weak interaction. Also exemplary shown in Fig. 7. So we find a dependence of α_{weak}^6 for this kind of processes. Since this VV production is a purly EW process it can be defined as background for the extraction of dimension six limits in the inclusive phase space for the dominating QCD VV production. And it is still background for the effect of dimension eight operators but also needed to be studied in the VBS phase space because we don't know the impact of dimension six EFTs operators in this phase space.

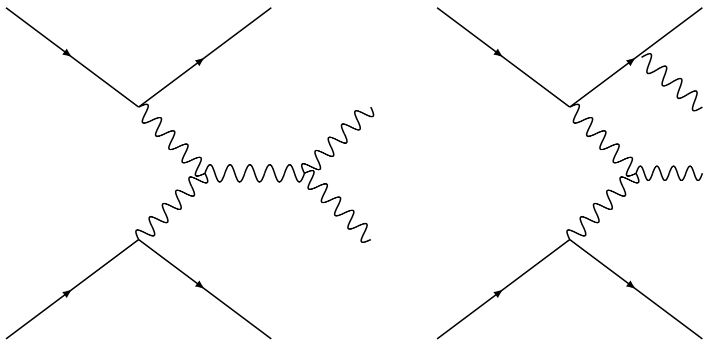

Figure 7 – Example for a EW mediated VV production

Chapter 3

The ATLAS detector

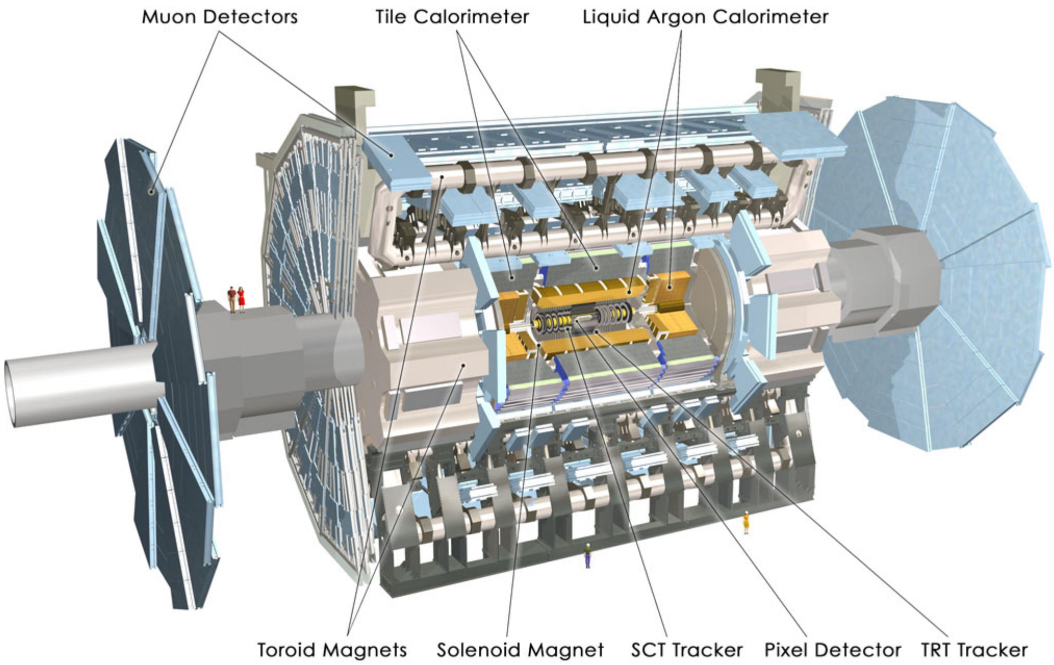

Figure 8 – Schematic structure of the ATLAS detector [8]

.

The ATLAS detector on which the Monte Carlo generated data of the analysis are based is located in the largest particle accelerator in the world, the Large Hadron Collider (LHC). Proton-proton collisions take place in it. The LHC has a circumference of $27\,km$ and is designed for a center of mass energy of up to $\sqrt{s} = 14\,TeV$. However, during the past year it was operated with a center of mass energy of $\sqrt{s} = 7\,TeV$, $\sqrt{s} = 8\,TeV$ and latest data were recorded with $\sqrt{s} = 13\,TeV$. The accelerator is located $100\,m$ underground. The ATLAS detector itself is $44\,m$ long, $25\,m$ high and weighs $6.4 \cdot 10^6\,kg$. A schematic representation is shown in figure 8 and consists of several systems, which are briefly explained below. More detailed information can be found in [10].

3.1 Magnetic System

The magnet system of the ATLAS detector consists of the solenoid system and the toroid system. The former is used to determine the transverse momentum of charged particles and is located between the inner detector and the electromagnetic calorimeter. Its magnetic field is nearly homogeneous in the range of $|\eta| < 2.7$ and has a strength of $2\,T$. The toroid system consists of one central and two end cap toroids. The central toroid serves to determine the transverse momentum of muons and can cause a trajectory curvature of $2-6\,mT$ in a range of $0 \leq |\eta| \leq 1.3$. The end cap toroids enclose the hadronic and the electromagnetic calorimeter. In the range $1.6 \leq |\eta| \leq 2.7$ they have a curvature strength of $4-8\,mT$ [10].

3.2 Inner detector

The inner detector can be divided into three parts: the Silicon Pixel Detector, the Silicon Strip Detector (SCT) and the Transition Radiation Tracker (TRT). The first two are semiconductor detectors. The pixel detector is the innermost track detector. It is used in a range up to $|\eta| = 2.5$ to detect vertices. The SCT is divided into detector strips and serves a range of $1.4 \leq |\eta| \leq 2.5$. The third sub-detector, the TRT, on the other hand, consists of gas-filled drift tubes and can be used in addition to the normal track detection also to detect transitional radiation [10].

3.3 Calorimeter

The calorimeter system consists of a hadronic and an electromagnetic calorimeter. With this system, the energy of particles with very high energy in a range up to $|\eta| = 4.9$ can be measured. The electromagnetic calorimeter is a sandwich calorimeter consisting of a central part and two end caps. The central part reaches up to $|\eta| = 1.475$ and the end caps cover the range $1.375 \leq |\eta| \leq 3.2$. Lead is used as the absorber material and liquid argon (LAr) as the active material. The hadronic calorimeter surrounds the electromagnetic calorimeter up to $|\eta| = 4.9$ and is composed of three components: a plate calorimeter, an end-cap calorimeter and a forward calorimeter. The plate calorimeter is a sandwich calorimeter with iron as absorber material ($|\eta| < 1.7$). Here the luminescence of the scintillator is used as a signal. The end cap measures in the range of $1.5 < |\eta| < 3.2$ and is also a sandwich calorimeter, where again iron is used for absorption and LAr as active material. A part of the absorber material of the forward calorimeter consists of copper and two other parts of tungsten. The active material is also LAr. But these parts are thinner than in the other calorimeters, because the forward calorimeter is very close to the beam and therefore has a high particle flux. Which means that this calorimeter has to be especially hard. The measuring range is as follows $3.1 \leq |\eta| \leq 4.9$ [10].

3.4 Muon system

The muon system consists of four parts, the Monitored Drift Tubes (MDT), the Cathode Strip Chambers (CSC), the Resistive Plate Chambers (RPC) and the Thin Gap Chambers (TGC). It is used to determine the transverse momentum of muons from some GeV up to $3\,TeV$ and can measure pseudo-rapidity up to $|\eta| = 2.7$. Drift tubes are used in the MDT. The CSC and the RPC are constructed as multi-wire proportional chambers and serve as triggers in the central muon system and in the end cap areas [10].

3.5 Trigger system

The event rate in the ATLAS detector can reach up to $40\,MHz$. However, since the available storage space is significantly below this value and approx. $1.5\,MB$ is required per event, only 1 event of 100000 can be recorded. Therefore, good triggers must be used which decide on the recording of an event and reduce the event rate significantly. This reduction allows a more time-intensive and therefore more accurate analysis in the following steps. The online trigger system consists of the following three components:

- **Level 1:** This is a hardware trigger which is supported by user-defined electronics. The Central Trigger Processor (CTP) generates Level 1 acceptance based on information from the calorimeters, muon system, and forward detectors, enabling further processing of the data. Taking into account the measurements of transverse and missing energy regions of interest (ROIs) are selected for further evaluation. The event rate is reduced within $2.5\,\mu s$ from $40\,MHz$ to $75\,kHz$.

- **Level 2:** The previously defined ROIs are now examined more closely, using the information from all detectors. For the reduction of the event rate from $75\,kHz$ to $1\,kHz$ $40\,ms$ are available.

- **Level 3:** At the last trigger level, offline algorithms are used within the of the online framework structure. Now all available data can be used. This reduces the event rate from $40\,kHz$ to $200\,Hz$ within $4s$ [10].

Chapter 4

Simulation of $W^{\pm}Z$ production

To study anomalous triple gauge couplings in the VBS phase space we decide to use $W^{\pm}Z$ as the two vector bosons that we discussed in section 2.4 and 2.5. In this chapter we will explain the simulation of the $W^{\pm}Z$ as QCD and EW mediated production.

4.1 Event generation using Monte Carlo simulation

First of all to simulate a process of particle interaction a Monte Carlo simulation is used. The reason for this is that if we have a look on collisions like the one that occurs in the ATLAS detector (section 3) we can't give a statement about the processes that will happen. The only information that we have about the known processes is the probability with which they will take place. This probability is given by the cross section σ of a process. So to simulate a process we need kind of algorithm that produce random events of these process with a weighting of the probability density for this processes. This can be implemented with a Monte Carlo simulation. Algorithms which calculate approximate results by repeated random sampling are called Monte Carlo method [23].
So if we have a look more in detail what is needed to simulated an event. We need three information to calculate it:

- The parton level cross section $\hat{\sigma}$ which can be calculated by the matrix element $\mathcal{A}$
- The parton density function f which is determined by the type of the parton and is completely process independent

- The phase space (ps) integral which depend on the parton energy $\hat{s} = x_1 x_2 s$ and so also on the collision energy of the collider s

So with this information we get the following formula that needs to be calculated [16]:

$$\sigma = \int \hat{\sigma}_{ab \to X} (\hat{s}, ...) \, f_a (x_1) \, f_b (x_2) \, dx_1 dx_2 d\Phi_{\text{ps}} \tag{4.1}$$

The expectation value of this integral is approximate determined with a Monte Carlo method calculation [7]:

$$\langle \sigma (x_1, x_2, ...) \rangle = \int \sigma (x_1, x_2, ...) \, \varphi (x_1, x_2, ...) \, dx_1 dx_2 ... \tag{4.2}$$

$$\approx \frac{1}{N} \sum_{i}^{N} \sigma ((x_1, x_2, ...)_i) \pm \sqrt{\frac{\langle \sigma (x_1, x_2, ...)^2 \rangle - \langle \sigma (x_1, x_2, ...) \rangle^2}{N}} \tag{4.3}$$

To make the calculation much more efficient several methods could be used. One of them is to use *Importance Sampling*. Where the algorithm learns during the run and builds a step-function approximation. More about this method can be found here [17]. The main idea of a Monte Carlo simulation is to use a random number between zero and one and transform it to given a distribution scaled with the determined probability density. So there are two possible ways to get an event with a predetermined distribution.
For the first one the density function $\varphi (x)$ has to be confined $0 < \varphi (x) < B (x)$. Then we take a random number r_1 in the interval $[0, 1)$ and project it into the range of $\varphi (x)$. For the given the range $[a, b]$ we get

$$x = a + (b - a) \, r \tag{4.4}$$

The value of x will be accepted if r has a probability of $\leq \frac{\varphi(x)}{B(x)}$. If not x and r_1 will be quashed and the algorithm start with a new r. This method is called rejection method. Here not all generated numbers will be used but the rejection method is useful if no transformation function $f (x)$ for $\varphi (x)$ exists or is to costly to calculate [24].
The other algorithm to generate random numbers with a pretended distribution is called inverse transform sampling. There the density function $\varphi (x)$ doesn't need to be confined but we need a transformation function $f (x) = y$. This function has to be bijective with $x = f (y)^{-1}$ and $\varphi (y)$ needs to be equally distributed so that the following applies:

$$\varphi (x) = \varphi (y) \left| \frac{dy}{dx} \right| = c \left| \frac{df \, (x)}{dx} \right| \tag{4.5}$$

with these transformation function we can randomly choose y in the range $[0,1)$ and calculate x with the inverse function $x = \varphi(y)^{-1}$ [24].
With a Monte Carlo simulation we want to generate the processes of section 2.5.2.

4.2 Simulated samples

This study about the anomalous gauge couplings is specified on the $W^{\pm}Z$ channel with ATLAS. So the vector bosons of the processes described in section 2.5.2 are chosen to be $W^{\pm}Z$ and are simulated for possible measurements in the ATLAS detector. Furthermore for the $W^{\pm}Z$ channel we have chosen the fully leptonic decay of the gauge bosons. As shown in section 2.2.1 the branching ratio for this decay is small but the signal that is recorded in the detector for this decay mode is clear. And therefore we have much less background processes as in any kind of hadronic decay.

4.2.1 The QCD mediated sample

The QCD mediated production of $W^{\pm}Z$ and fully leptonic decay is generated as following:

$$pp \to W^{\pm}Z \to \ell^{-}\ell^{+}\ell^{\pm}\nu \tag{4.6}$$

with up to two additional jets in the matrix element so that this sample could also be studied in VBS phase space. The intermediated step makes sure that generated events peaks to the mass of $W^{\pm}Z$. Finally the events are merged to avoid double counting after the showering. Furthermore we assumed the up, down, charm, strange and bottom quark as massless as well as the electrons and muons. The event generation started with the requirements shown in Tab 6.

Variable	Cut
min p_T jets	$20\,GeV$
min p_T charged leptons	$10\,GeV$
min p_T at least one heavy final state	$2\,GeV$
max η jets	5.5
max η charged leptons	3.0
min ΔR_{jj} between jets	0.3
min $\Delta R_{\ell\ell}$ between leptons	0.2
min $\Delta R_{\ell j}$ between jet and lepton	0.2
min $\Delta R_{\gamma j}$ between γ and lepton	0.1
min $M_{\ell\ell}$ lepton pair	$4\,GeV$

Table 6 – Requirements for the QCD mediated $W^{\pm}Z$ event simulation with fully leptonic decay

The complete process was separated in four subprocesses for W^+, W^- and same flavour as well as opposite flavor leptons just for technical reasons. The process and parameter cards are shown in Fig. 34 and Fig. 35.

4.2.2 The EW mediated sample

The EW mediated production of $W^{\pm}Z$ and fully leptonic decay is generated as following:

$$pp \rightarrow W^{\pm}Z \rightarrow \ell^-\ell^+\ell^{\pm}\nu jj \tag{4.7}$$

The approximations with massless quarks and leptons, the intermediated step from pp to $W^{\pm}Z$ and the subsequent decay to leptons are the same for the QCD mediated $W^{\pm}Z$ production. The important difference is the requirement that no QCD vertex appears.The event generation include the requirements shown in Tab 7.

Variable	Cut
min p_T jets	$15\,GeV$
min p_T charged leptons	$4\,GeV$
min p_T at least one heavy final state	$2\,GeV$
max η jets	5.5
max η charged leptons	5.2
min ΔR_{jj} between jets	0.0
min $\Delta R_{\ell\ell}$ between leptons	0.2
min $\Delta R_{\ell j}$ between jet and lepton	0.2
min $\Delta R_{\gamma j}$ between γ and lepton	0.1
min $M_{\ell\ell}$ lepton pair	$4\,GeV$

Table 7 – Requirements for the EW mediated $W^{\pm}$ event simulation with fully leptonic decay

For the EW mediated $W^{\pm}Z$ production b quarks are excluded. Therefore all events produced with a b quark would be removed so we decided to not generate them at all. The reason for a exclusion of b quarks is that we would produce a lot of background events which doesn't came from a Vector Boson Scattering process as we see in Fig. 9.

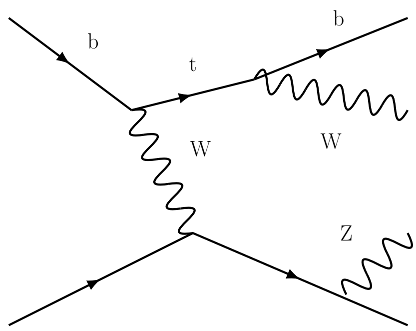

Figure 9 – Background event with an involved b quark for electroweak mediated triple gauge coupling

.

By excluding b quarks also Vector Boson Scattering processes are removed but these cut removes significantly background.

4.2.3 Simulation, object and event selection

The events of the processes of QCD and EW mediated $W^{\pm}Z$ production are simulated with the MadGraph generator interface with PYTHIA 8 for the modeling of the parton shower, hadronization and underlying event. Therefore MadGraph

2.6.5 is used for the phase space integration and MadGraph 2.6.2 for the events generation. The events are generated for a center of mass energy of $\sqrt{s} = 13\,TeV$ and are finally scaled to a integrated luminosity of $36.1\,fb^{-1}$. The simulation is done for truth level which means that we didn't simulate the reconstruction of the events by the detector (section 3) over the top of the generated events. But the cuts for $|\eta|$ are motivated by the range in that the detector is able to measure a signal. τ leptons are not included. The object and the so called total phase space are then defined as:

- energy and momentum of γ, and e^+e^- pairs in a cone of $R = 0.1$ around leptons are added up to a single electron object
- no τ lepton in the events
- exactly three leptons in each event while two of them have the same flavour and opposite charge ($\ell_1^+ \ell_2^- \ell_3^\pm$)
- at least one neutrino in each event which fits to the flavour of $\ell_{W^\pm}^3$
- for jets objects: $p_t \geq 25\,GeV$ and $|\eta| \leq 4.5$
- jet and lepton objects have to be isolated in a cone of $R = 0.3$
- the lepton objects ℓ_1, ℓ_2 and ℓ_1 are associated with the $W^\pm$ and Z bosons with an algorithmic approach called *resonant shape* [4]
- mass window of Z: $81.1876\,GeV < m_Z < 101.1876\,GeV$
- p_T for ℓ_1 and $\ell_2 > 15\,GeV$
- p_T for $\ell_3 > 20\,GeV$
- η for leptons > 2.5
- missing $E_T > 30\,GeV$
- isolation of ℓ_1 and ℓ_2 $\Delta R > 0.3$

This objects in the fiducial phase space we can be used for a analysis in the inclusive and VBS phase space.

4.2.4 Dimension six parameters

To produce the anomalous triple gauge couplings by the dimension six EFTs operators of an effective field theory (section 2.3) we used the *EWdim6* model. Information about the *EWdim6* can be found in [6]. With these model it is possible to simulate not only events with any value of the dimension six parameters (section 2.3.1) but also SM, interference, quadratic and cross term events separately how we explained in section 2.31. This can be done by a new physics parameter *NP* which has different values for different desired coupling orders combination [14]. The value of the dimension six parameters that are investigated are chosen as the $1D$ limits measured in the $W^{\pm}Z$ boson pair production with ATLAS by the combined data of $\sqrt{s} = 8\,TeV$ and $\sqrt{s} = 13\,TeV$:

Coupling	Observed $[TeV^{-2}]$
c_w/Λ^2	$[-3.6; 7.3]$
c_{www}/Λ^2	$[-3.3; 3.2]$
c_b/Λ^2	$[-253; 136]$

Table 8 – 1D limits for dimension six parameters measured in the $W^{\pm}Z$ boson pair production and fully leptonic decay with ATLAS data of $\sqrt{s} = 13\,TeV$ [18]

Since we just concentrate on $1D$ limits the cross terms described in section 2.31 can be canceled by setting $c_i c_j/\Lambda^4 = 0$. While the interference and quadratic parts are just generated for the positive limits, the whole process that includes the standard model, interference and quadratic terms are generated for the upper and lower $1D$ limits.

Combining the new physics contributions

The separate parts of the standard model triple gauge couplings and the anomalous triple gauge coupling effects can now be combined to obtain the complete process. Since $1D$ limits are used , only one parameter is modified at the time and therefore cross terms are not existing.

$$S_{sum} = S_{SM} + S_{interf} + S_{quad} \tag{4.8}$$

The separate generated samples S can be scaled to any choice of dimension six parameters. So with the separate samples $S_{SM,i}$, $S_{interf,i}$ and $S_{quad,i}$ for a aTGC point c_i/Λ^2 we get the sample S_j for the c_j/Λ^2 value :

$$S_{sum,j} = S_{SM} + \frac{c_j}{c_i} S_{interf,i} + \left(\frac{c_j}{c_i}\right)^2 S_{quad,i} \tag{4.9}$$

Chapter 5

Analysis

As already mentioned in Chapter 2.3.2 the study of Vector Boson Scattering (VBS) process is essential and only accessible for the first time at the LHC now. VBS is characterized at tree level by the exchange of weak gauge bosons between two quarks or a quark and an anti- quark, which gives us direct access to both triple and quartic gauge couplings. Since this is a purely electroweak process, it has a relatively small cross-section at LHC where the large QCD backgrounds dominate everywhere.

In this analysis we focus on the $W^{\pm}Z$ channel and look at the effects of dimension six EFTs operators affecting the QCD and EW mediated production at LHC. In particular, we want to see the effects of the dimension six EFTs operators in the total cross section and differential distributions. Two phase spaces are studied the inclusive and VBS defined in sections 2.4 and 2.5 respectively. The starting point of the study are the best limits obtained in dimension six EFTs operators by looking at the $W^{\pm}Z$ channel using ATLAS data. The limits used as a reference are the so called one dimensional limits (1D). The 1D limits are obtained by allowing only one EFT parameter to differ from the SM. The data is then compared with the 1D EFT model any difference between the data and the SM is attributed to that single parameter. Since this study is on the same channel as the calculation of the limits that are used, we can basically take any of the parameters at the limit value and do a sensible statement about the impact of dimension six parameters in the inclusive and most of all in the VBS phase space by just looking at one of these parameters. The effects of any of the other parameters at the limit value should by the definition have effects of roughly the same size.

5.1 Validation of the samples

In order to validate if the simulated samples that are described in 4.2 can be combined as discussed in section 4.2.4 a closure test was performed. For the closure test several samples generated with aTGC effects (full) were compared with the sum of the separated samples SM, interference with the SM and quadratic aTGC effects (sum of SM and dim6). Figures. 10 to 12 show the closure test in two different phase spaces. Since we want to study the impact of the aTGCs effects in the VBS phase space, a good closure of the samples in the VBS phase space is important. The figures on the left side of the page correspond to the inclusive WZ phase space and the figures on the right side correspond to the VBS phase space. Figures 10, 11, 14 and 13 show the closure for the QCD mediated $W^{\pm}Z$ production while Figures 12 and 15 show the closure for the EW mediated production.

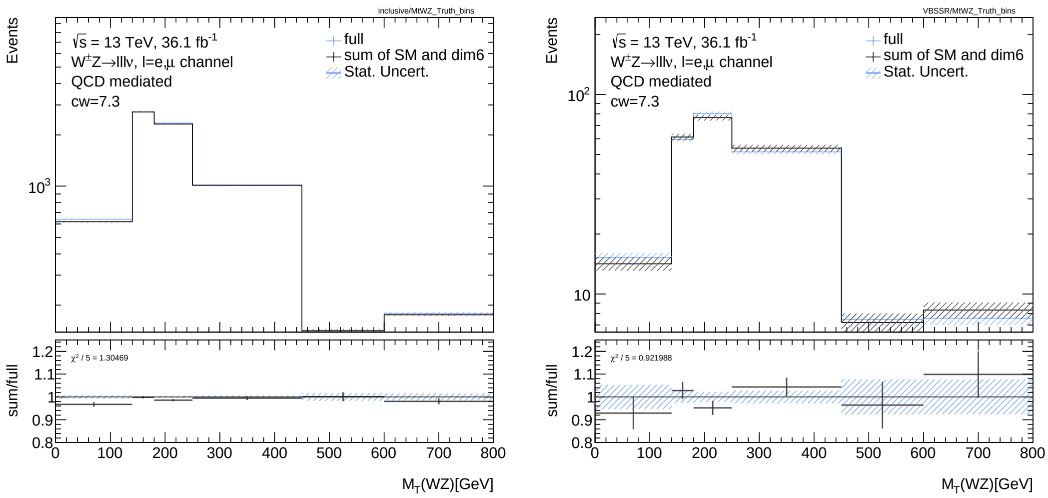

Figure 10 – Comparsion between the full generated aTGC sample and separated SM, interference with the SM and aTGC effects and quadratic aTGC effects samples for QCD mediated $W^{\pm}Z$ production and fully leptonic decay with the dimension six parameter $c_w = 7.3$ left in the inclusive phase space and right in the VBS phase space.

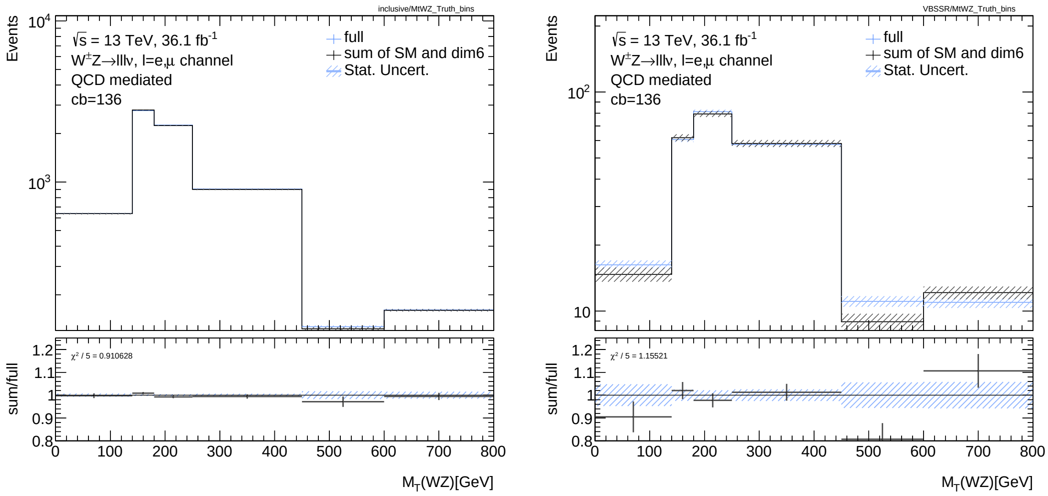

Figure 11 – Comparsion between the full generated aTGC sample and separated SM, interference with the SM and aTGC effects and quadratic aTGC effects samples for QCD mediated $W^{\pm}Z$ production and fully leptonic decay with the dimension six parameter $c_b = 136$ left in the inclusive phase space and right in the VBS phase space.

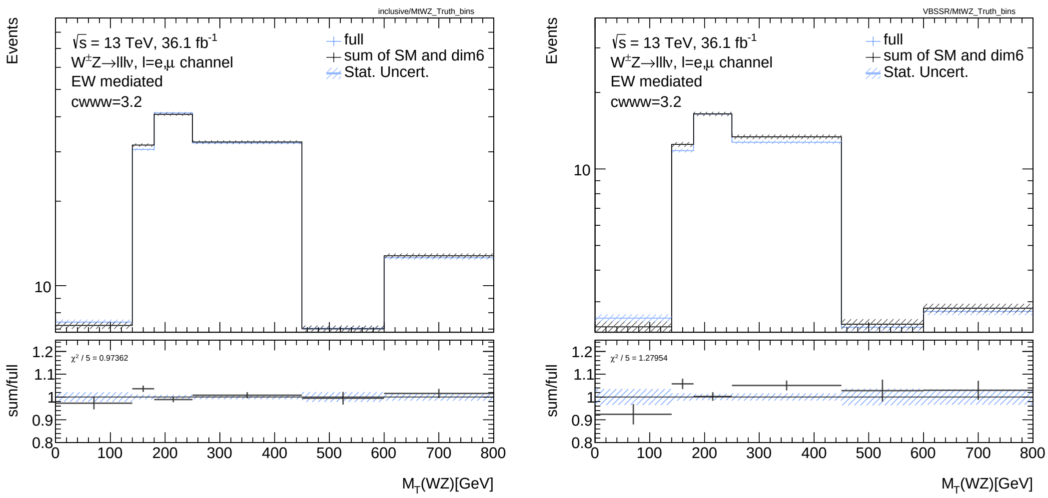

Figure 12 – Comparsion between the full generated aTGC sample and separated SM, interference with the SM and aTGC effects and quadratic aTGC effects samples for EW mediated $W^{\pm}Z$ production and fully leptonic decay with the dimension six parameter $c_{www} = 3.2$ left in the inclusive phase space and right in the VBS phase space.

The simulation of the SM, interference of the dimension six EFTs operator $\mathcal{O}_w/\Lambda^2$ and the quadratic part of $\mathcal{O}_w/\Lambda^2$ for the QCD mediated $W^{\pm}Z$ production fits very well with the simulation of the full process in the inclusive phase and also in the VBS phase space with consideration to the statistical uncertainties. Also the test of the simulation for the EW mediated $W^{\pm}Z$ production looks fine. So the separation of the samples is considered validated.

Using the separated contributions also allow us to scale the different contributions to any value of the aTGC parameter. Fig. 13 to 15 where built by scaling the interference and quadratic term to the lower limits previously extracted by the ATLAS collaboration. The scaled contributions are compared with a full sample at the same values.

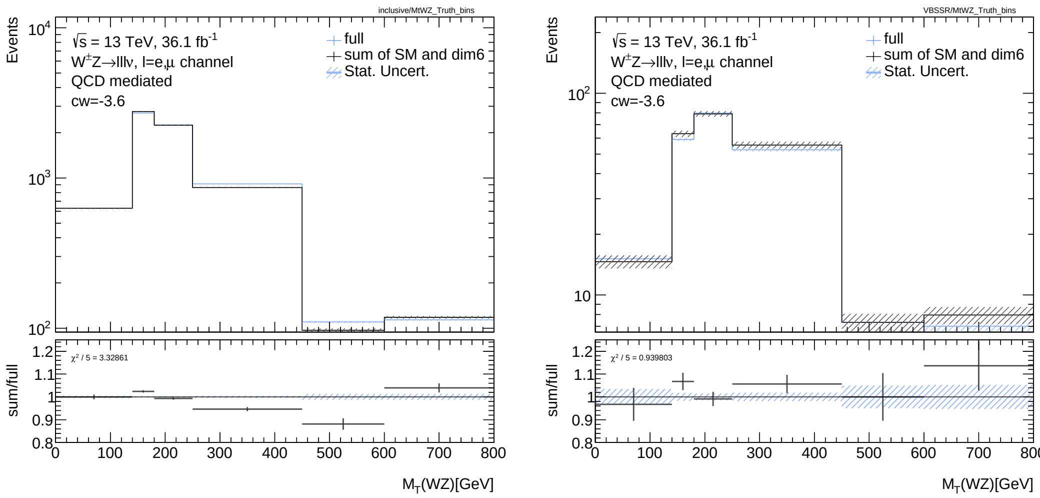

Figure 13 – Comparsion between the full generated aTGC sample with the dimension 6 parameter $c_w = -3.6$ and separated SM, interference with the SM and aTGC effects and quadratic aTGC effects samples for QCD mediated $W^{\pm}Z$ production and fully leptonic decay scaled to the dimension six parameter $c_w = -3.6$ left in the inclusive phase space and right in the VBS phase space.

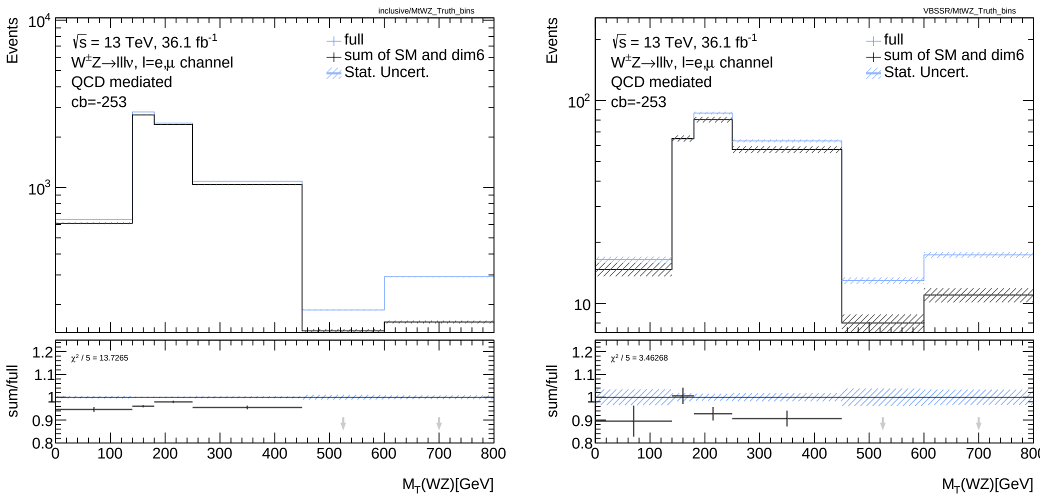

Figure 14 – Comparsion between the full generated aTGC sample with the dimension 6 parameter $c_b = -253$ and separated SM, interference with the SM and aTGC effects and quadratic aTGC effects samples for QCD mediated $W^{\pm}Z$ production and fully leptonic decay scaled to the dimension six parameter $c_b = -253$ left in the inclusive phase space and right in the VBS phase space.

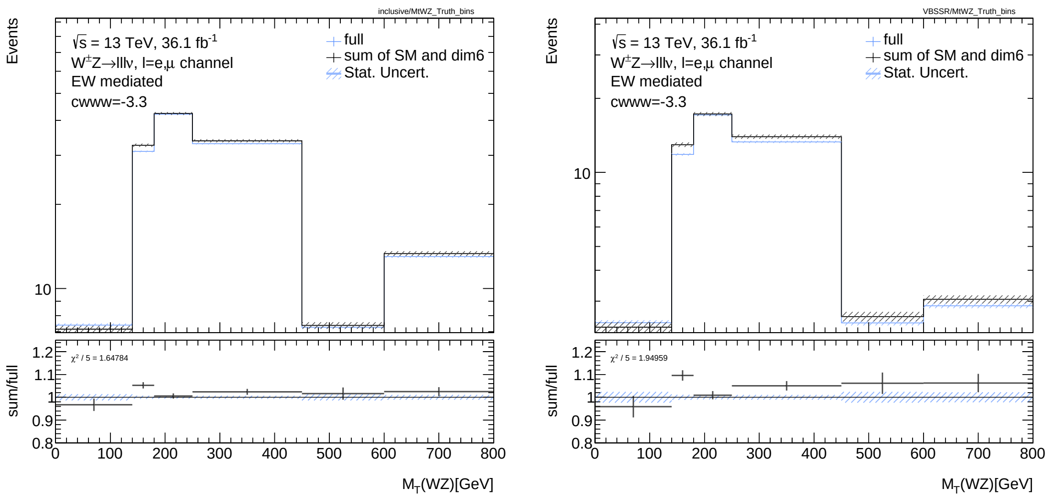

Figure 15 – Comparsion between the full generated aTGC sample with the dimension 6 parameter $c_{www} = -3.3$ and separated SM, interference with the SM and aTGC effects and quadratic aTGC effects samples for EW mediated $W^{\pm}Z$ production and fully leptonic decay scaled to the dimension six parameter $c_{www} = -3.3$ left in the inclusive phase space and right in the VBS phase space.

The sum of the separated simulation scaled to the lower limits also agrees with the fully generated $W^{\pm}Z$ production for the QCD mediated process with c_w and for the EW mediated process with c_{www}. Even if the limits aren't symmetric. The QCD mediated $W^{\pm}Z$ production with c_b on the other hand do not show a good agreement (Fig. 14). There are two possible reasons for these result. First the $W^{\pm}Z$ channel with fully leptonic decay is not very sensitive to the $\mathcal{O}_b$ operator. This means that the values used in this study for c_b are quite large. Since a we have to scale from $c_b = 136$ to $c_b = -253$ small differences are magnified. The second reason could come from the merging procedure used in the QCD simulation to avoid double counting of the events. When the samples were generated a bug in the estimation for the cross section calculation on generator level in PYTHIA was found. It can be that the cross section for the discussed sample increases after the merging instead of the assumed decreasing for the interference and quadratic effects. This still needs to be fixed by experts and could be here at the origin of the bad result of Fig. 11. Due to the low sensitivity and the closure problem with the sample containing non zero c_b parameter this analysis will focus only on the QCD mediated $W^{\pm}Z$ production with the additional operator $\mathcal{O}_w$ and the EW mediated $W^{\pm}Z$ production with the additional operator $\mathcal{O}_{www}$.

5.2 Impact of dimension six EFTs operators on physical observables

Adding dimension six EFTs operators to the SM Lagrangian in the EFT context can modify the cross section and kinematic distributions of the $W^{\pm}Z$ production. The transverse momentum of $W^{\pm}$, the transverse momentum of Z and the transverse mass of $W^{\pm}Z$ system are sensitive to the anomalous triple gauge coupling caused by dimension six EFTs operators. But there are also observables that aren't sensitive to the impact of dimension six EFTs operators like the mass of the two tagging jets or $\Delta\eta$ between $W^{\pm}$ and Z. This is already shown in previous studies in the inclusive phase space like [3].
Since we want to study the effect of dimension six EFTs operators in the VBS phase space, we will have a look to the observables sensitive to aTGCs in the VBS phase space. The EW mediated $W^{\pm}Z$ production so far was considered to do not be sensitive to the additional impact of dimension six EFTs operators in the inclusive phase space. This is the reason why the EW mediated $W^{\pm}Z$ production was in all studies considered as background for the extraction of limits for the dimension six parameters c_i/Λ^2. But diagrams including TGCs are also part of the EW mediated production and the impact of the dimension six EFTs operators in the EW $W^{\pm}Z$ mediated production was never investigated in the VBS phase space before.

Fig. 16 to 20 show some distributions in the inclusive phase space on the left side and in the VBS phase space on the right side for the QCD mediated $W^{\pm}Z$ production and the influence of the $\mathcal{O}_w$ operator. The contributions of the EW mediated $W^{\pm}Z$ production with the influence of the $\mathcal{O}_{www}$ operator are shown in Fig. 21 to 25. On the figures the impact of only one modified dimension six parameter at the time was test. The reason for this is that we are taking as a reference the channel dependent 1D limits provided by the collaboration. Combined effect of two or more parameters at the time are also possible and were not explored yet.

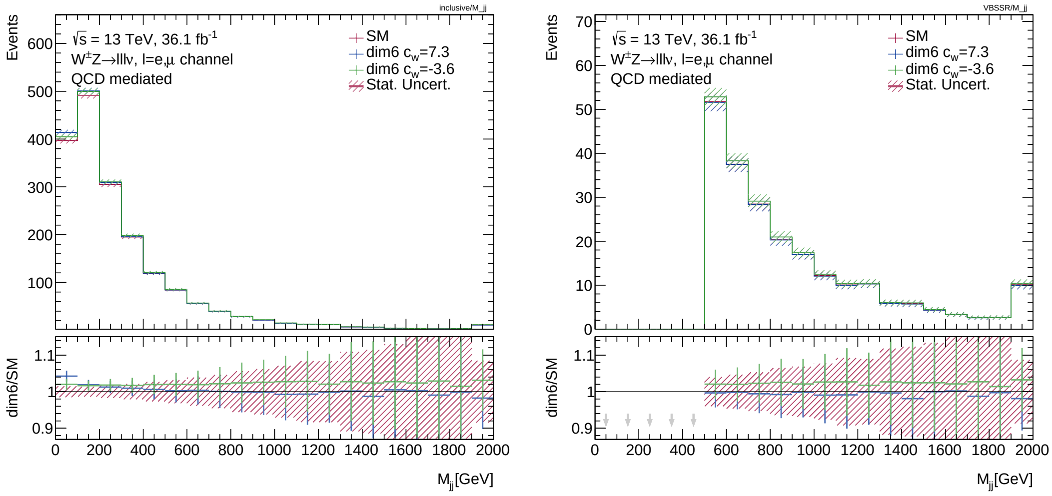

Figure 16 – The impact for the dimension six EFTs operator $\mathcal{O}_w$ with $cw = 7.3$ and $c_w = -3.6$ of the mass of the tagging jets in the inclusive phase space (left) and in the VBS phase space (right) for QCD mediated $W^{\pm}Z$ production and fully leptonic decay.

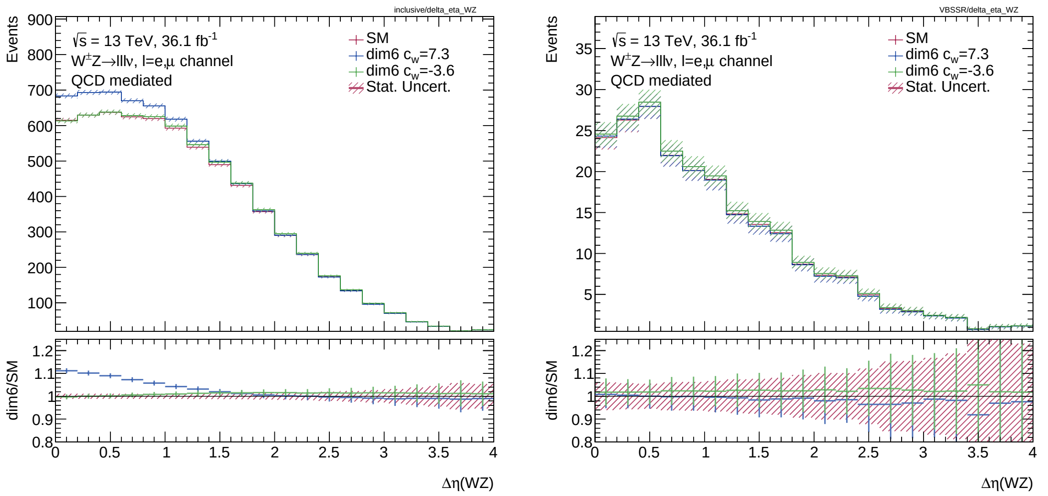

Figure 17 – The impact for the dimension six EFTs operator $\mathcal{O}_w$ with $c_w = 7.3$ and $c_w = -3.6$ of the $\Delta\eta$ between $W^{\pm}$ and Z in the inclusive phase space (left) and in the VBS phase space (right) for QCD mediated $W^{\pm}Z$ production and fully leptonic decay.

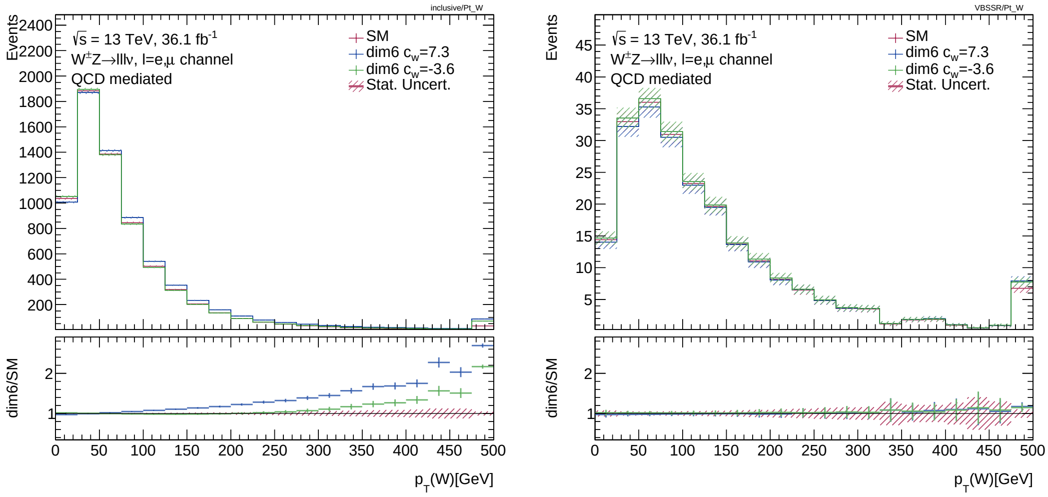

Figure 18 – The impact for the dimension six EFTs operator $\mathcal{O}_w$ with $cw = 7.3$ and $c_w = -3.6$ of the transverse momentum of $W^{\pm}$ in the inclusive phase space (left) and in the VBS phase space (right) for QCD mediated $W^{\pm}Z$ production and fully leptonic decay.

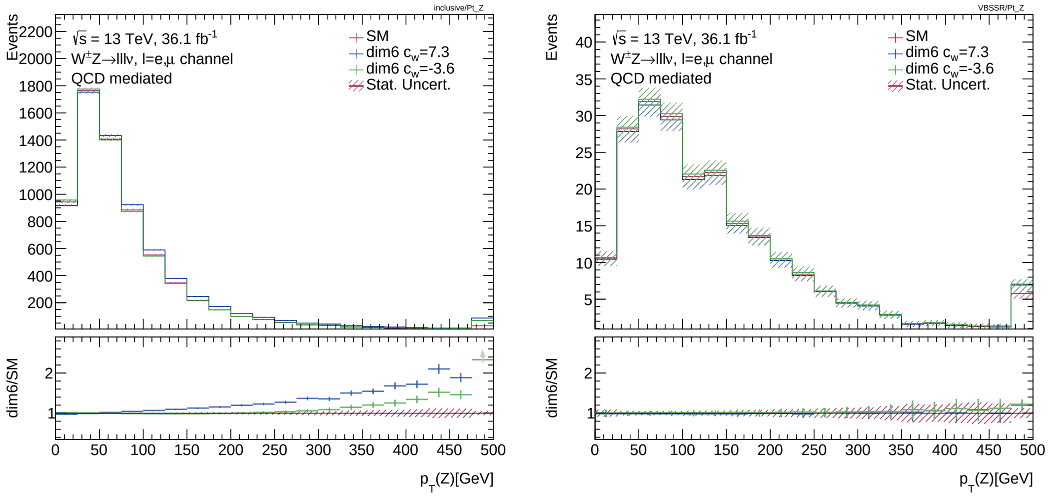

Figure 19 – The impact for the dimension six EFTs operator $\mathcal{O}_w$ with $cw = 7.3$ and $c_w = -3.6$ of the transverse momentum of $Z^{\pm}$ in the inclusive phase space (left) and in the VBS phase space (right) for QCD mediated $W^{\pm}Z$ production and fully leptonic decay.

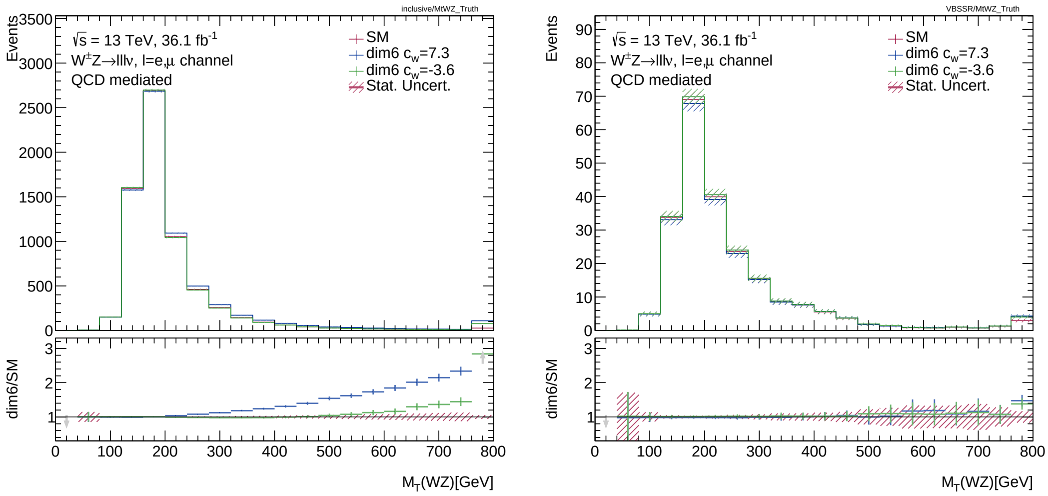

Figure 20 – The impact for the dimension six EFTs operator $\mathcal{O}_w$ with $cw = 7.3$ and $c_w = -3.6$ the transverse momentum of $W^{\pm}$ in the inclusive phase space (left) and in the VBS phase space (right) for QCD mediated $W^{\pm}Z$ production and fully leptonic decay.

From Fig. 16 to 20 we see that the mass of the tagging jets and $\Delta\eta$ between $W^{\pm}$ and Z aren't sensitive to anomalous triple gauge couplings. While the transverse momentum of $W^{\pm}$ and Z and the transverse mass of $W^{\pm}Z$ are sensitive. Being the transverse mass of $W^{\pm}Z$ the most sensitive observable for a study of dimension six EFTs operators in the inclusive and VBS phase space, see Fig.20. The transverse mass of $W^{\pm}Z$ was defined as

$$m_T^{W^{\pm}Z} = \sqrt{\left(\sum_{\ell} p_T^{\ell} + E_T^{\text{miss}}\right)^2 - \left[\left(\sum_{\ell} p_x^{\ell} + E_x^{\text{miss}}\right)^2 + \left(\sum_{\ell} p_y^{\ell} + E_y^{\text{miss}}\right)^2\right]} \quad (5.1)$$

To have a more impressive view to the impact of a dimension six EFTs operator for a QCD and EW mediated $W^{\pm}Z$ production the binning for the limits extraction of c_i/Λ^2 is used in Fig. 26 and 33.

In the VBS phase space most of the QCD mediated $W^{\pm}Z$ produced events are removed, what is completely reasonable since QCD mediated $W^{\pm}Z$ aren't produced by VBS. But also most of all dimension six EFTs operator effects are removed. The only visible effect is on the transverse momentum of $W^{\pm}Z$ in the overflow bin occurs a small deviation of the SM but fully covered by the statistical uncertainties. This behavior was never tested before and is a hint for the conclusion that the dimension six EFTs operators in a QCD mediated production doesn't give a notable impact to the in the VBS phase space studied.

Next we wanted to see the impact of dimension six EFTs operators in the inclusive phase space an the VBS phase space for a EW mediated $W^{\pm}Z$ production. The operator $\mathcal{O}_{www}$ was chosen for this test. Fig. 21 to 25 show some comparison for different observables.

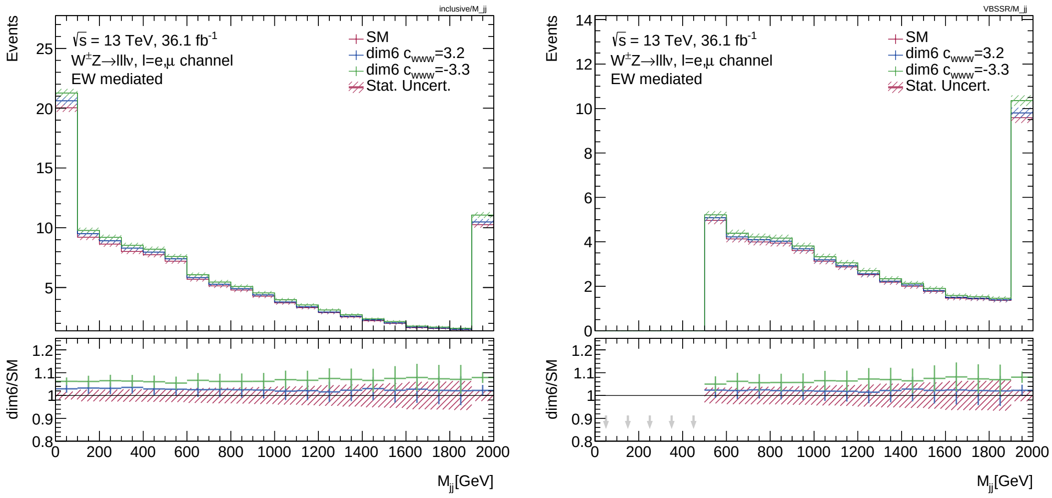

Figure 21 – The impact for the dimension six EFTs operator $\mathcal{O}_w$ with $c_{www} = 3.2$ and $c_{www} = -3.3$ of the mass of the tagging jets in the inclusive phase space (left) and in the VBS phase space (right) for EW mediated $W^{\pm}Z$ production and fully leptonic decay.

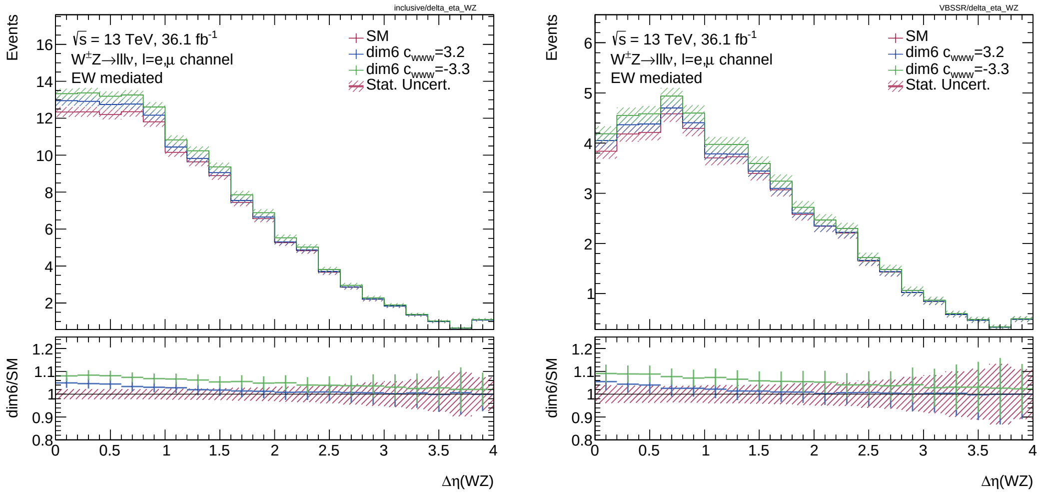

Figure 22 – The impact for the dimension six EFTs operator $\mathcal{O}_w$ with $c_{www} = 3.2$ and $c_{www} = -3.3$ of the $\Delta\eta$ between $W^{\pm}$ and Z in the inclusive phase space (left) and in the VBS phase space (right) for EW mediated $W^{\pm}Z$ production and fully leptonic decay.

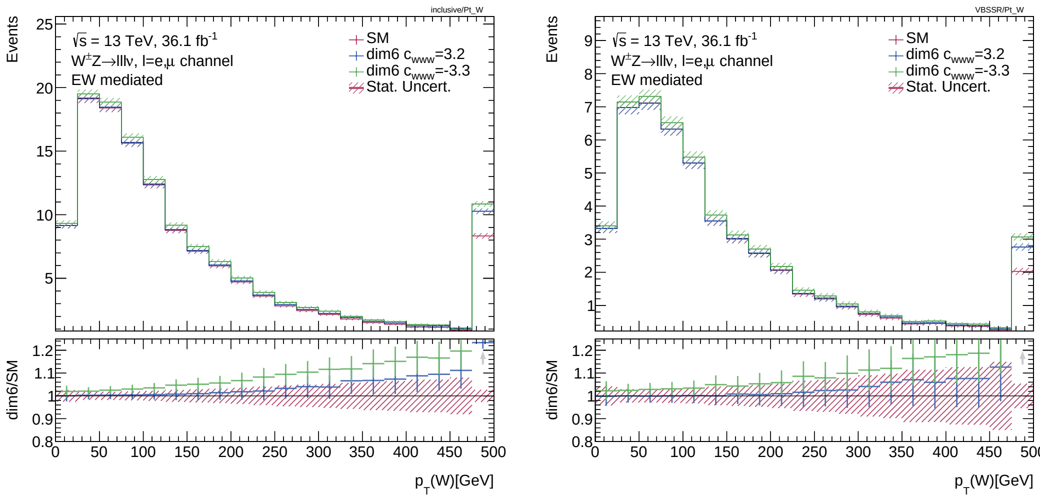

Figure 23 – The impact for the dimension six EFTs operator $\mathcal{O}_w$ with $c_{www} = 3.2$ and $c_{www} = -3.3$ of the transverse momentum of $W^{\pm}$ in the inclusive phase space (left) and in the VBS phase space (right) for EW mediated $W^{\pm}Z$ production and fully leptonic decay.

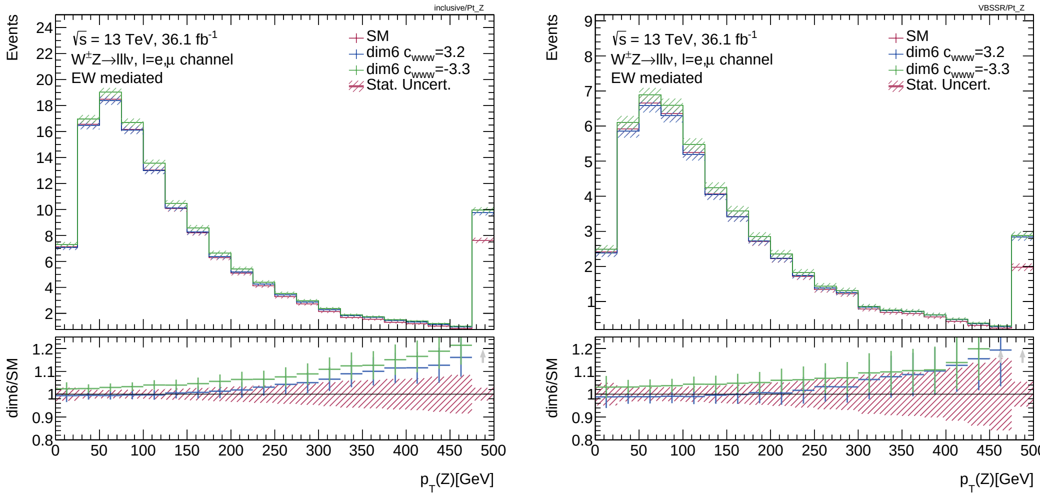

Figure 24 – The impact for the dimension six EFTs operator $\mathcal{O}_w$ with $c_{www} = 3.2$ and $c_{www} = -3.3$ of the transverse momentum of $Z^{\pm}$ in the inclusive phase space (left) and in the VBS phase space (right) for EW mediated $W^{\pm}Z$ production and fully leptonic decay.

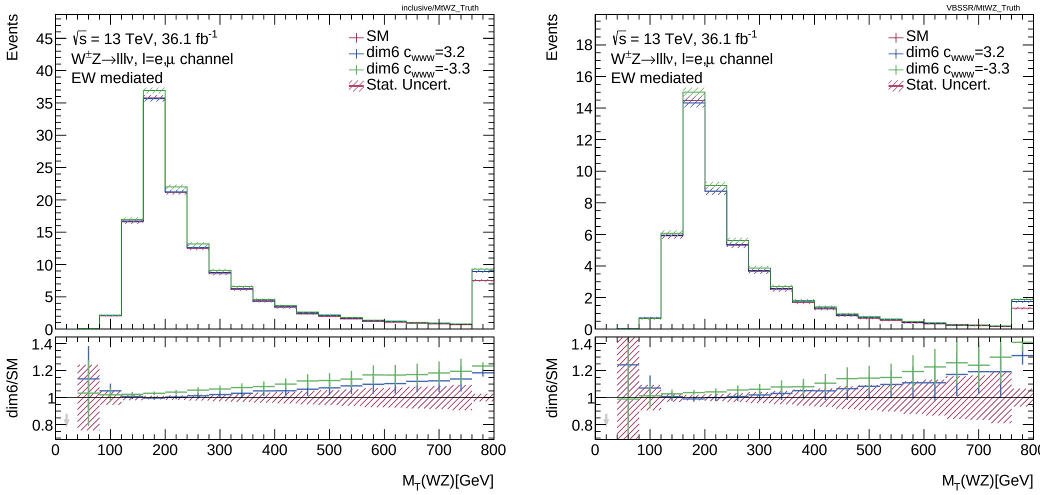

Figure 25 – The impact for the dimension six EFTs operator $\mathcal{O}_w$ with $c_{www} = 3.2$ and $c_{www} = -3.3$ of the transverse momentum of $W^{\pm}$ in the inclusive phase space (left) and in the VBS phase space (right) for EW mediated $W^{\pm}Z$ production and fully leptonic decay.

For the EW mediated $W^{\pm}Z$ production the influence of a dimension six EFTs operator can be seen has a small impact for all physical observables in the inclusive phase space. Since the EW contribution to the inclusive phase space is very small, the assumption made in previously version of the analysis of considering the EW mediated production of vector bosons as background for the dimension six limits should not have a big impact in the derived limits. In the VBS phase space on the other hand the impact is small but unlike in the inclusive phase space the

EW mediated production is more important in the VBS phase space. The impact of a dimension six EFTs operator in the VBS phase space has a sizable impact that should be considered while using the same phase space for dimension eight studies.

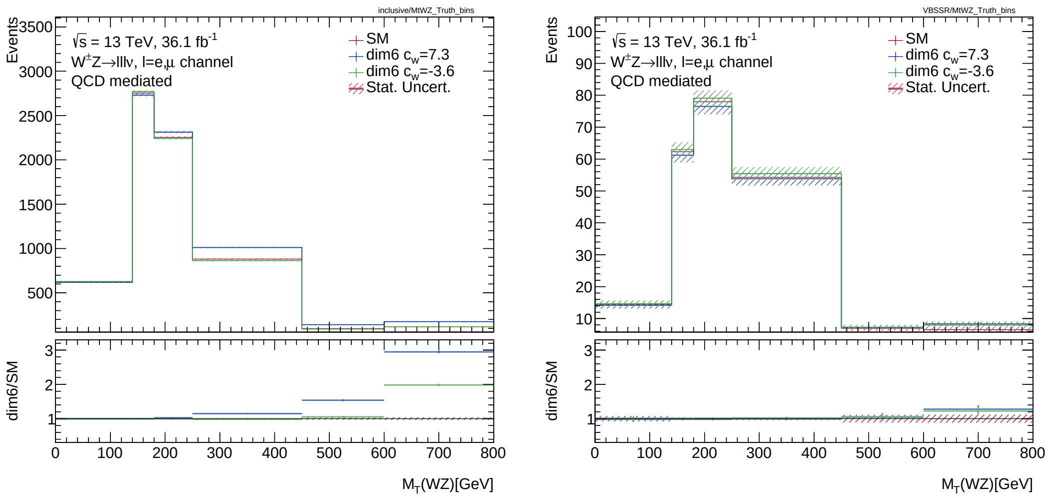

Figure 26 – The impact for the dimension six EFTs operator $\mathcal{O}_w$ with $cw = 7.3$ and $c_w = -3.6$ of the transverse momentum of $W^\pm$ in the inclusive phase space (left) and in the VBS phase space (right) for QCD mediated $W^\pm Z$ production and fully leptonic decay in the optimized binning for limit setting.

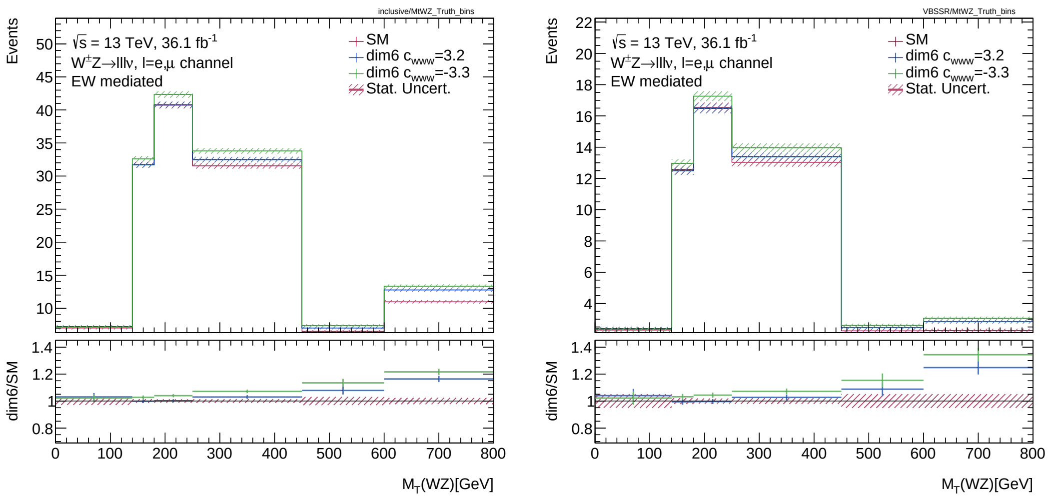

Figure 27 – The impact for the dimension six EFTs operator $\mathcal{O}_w$ with $c_{www} = 3.2$ and $c_{www} = -3.3$ of the transverse momentum of $W^\pm$ in the inclusive phase space (left) and in the VBS phase space (right) for EW mediated $W^\pm Z$ production and fully leptonic decay in the optimized binning for limit setting.

In Fig. 26 the strongly decreasing of a dimension six EFTs operator effect for QCD mediated $W^{\pm}Z$ production while the effect increases a little bit for EW mediated $W^{\pm}Z$ production (see Fig. 33) from the inclusive phase space to the VBS phase space. Thus the impact of anomalous triple gauge coupling effect caused by additional dimension six EFTs operators has the same order of magnitude for QCD and EW mediated $W^{\pm}Z$ production and so it is needed to give equal weight the both kinds of production in the VBS phase space.

5.2.1 Impact of dimension six EFTs operators on $M_T^{W^{\pm}Z}$

To study the behavior of the different contributions the shapes of the SM, the interference term and quadratic term in the inclusive phase space and VBS phase space Fig. 28 to Fig. 29 where made. All the figures show SM, interference and quadratic part normalized to their cross sections. In Tab. 9, the total number of events for the QCD mediated $W^{\pm}Z$ production with the dimension six EFTs operator $\mathcal{O}_w$ and $c_w = 7.3$ and for the EW mediated $W^{\pm}Z$ production with the dimension six EFTs operator $\mathcal{O}_{www}$ for $c_{www} = -3.6$ is given.
The $M_T^{W^{\pm}Z}$ distribution of the upper limits for the dimension six EFTs operators are only shown since the shape of the quadratic part of the dimension six EFTs operator stays the same for the lower limits and the shape of the interference part just switches its sign. To interpret the shapes correctly, we have to be careful about the impact of the interference between the SM and the dimension six EFTs operator. If the total impact (shown in Tab. 9) is negative, a positive part in the distribution means a negative impact here.

	inclusive phase space			VBS phase space		
events $[N]$	SM	interference	quadratic	SM	interference	quadratic
QCD	6663 ± 22	181 ± 2	146 ± 1	223 ± 5	-4 ± 1	3 ± 1
EW	129 ± 1	-3 ± 1	6 ± 1	49 ± 1	-1 ± 1	2 ± 1

Table 9 – Event numbers for the SM, interference between the SM and a dimension six operator and the quadratic effect of a dimension six operator with the dimension six operator $\mathcal{O}_w$ and $c_w = 7.3$ for the QCD mediated and $\mathcal{O}_{www}$ with $c_{www} = 3.2$ for the EW mediated $W^{\pm}Z$ production in the inclusive and VBS phase space.

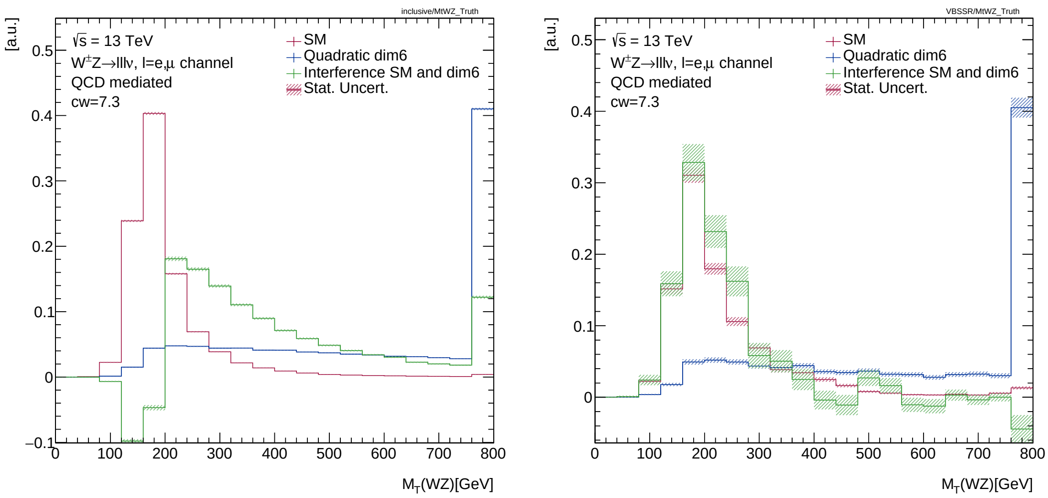

Figure 28 – The impact of the SM, interference part of the SM and the dimension six EFTs operator $\mathcal{O}_w$ and the quadratic part of the dimension six EFTs operator $\mathcal{O}_w$ with $cw = 7.3$ normalised the there number of events in the inclusive phase space (left) and in the VBS phase space (right) for QCD mediated $W^{\pm}Z$ production and fully leptonic decay.

In Fig. 28, the shape of interference of the SM and the dimension six EFTs operator in the inclusive phase space (left side) start with a negative impact with $\sim 15\%$ of its total impact and becomes positive at $M_T^{W^{\pm}Z} = 200\,GeV$. For $M_T^{W^{\pm}Z} = 200\,GeV$, the interference reaches the maximum ($\sim 18\%$) of its impact and behaves in a falling way until the overflow bin where still $\sim 15\%$ of the impact is left. The positive impact of the quadratic effect of the dimension six EFTs operator increases a little bit from the start up to $M_T^{W^{\pm}Z} = 200\,GeV$ and stays quite flat up to the overflow bin where the majority of the impact can be found with $\sim 40\%$. First, the interference between the SM and the dimension six EFTs operator dominates the additional impact. While the quadratic effect of the dimension six EFTs operator replaces the interference at increasing values of $M_T^{W^{\pm}Z}$ sometime in the inclusive phase space.
The shape of interference of the SM and the dimension six EFTs operator and the quadratic part of a dimension six EFTs operator in the VBS phase space is shown on the right side of Fig. 28. The VBS cuts (defined in section 2.5.1) remove the positive impact of the interference between the SM and dimension six EFTs operators for $M_T^{W^{\pm}Z} > 200\,GeV$ so that the impact is negative up to $400\,GeV$. Around $\sim 90\%$ of the whole interference impact can be found in this region. In the VBS phase space, the interference is almost always positive and flat distributed for $M_T^{W^{\pm}Z} \geq 400\,Gev$ but small ($\sim 10\%$) in comparison to the negative impact for $M_T^{W^{\pm}Z} < 400\,Gev$. While the shape of the quadratic part stays completely the same in the VBS phase space as in the inclusive phase space.

The amount of impact for the quadratic and interference part are nearly the same (see Tab. 9). Thus, the dominating part of the quadratic term starts earlier than in the inclusive phase space. Since the quadratic effect of a dimension six EFTs operator is still dominating for growing $M_T^{W^\pm Z}$ in the VBS phase space, we assume a positive impact earlier as in the inclusive phase space. Furthermore, the impact of dimension six EFTs operators relative to the impact of the SM decrease heavily from the inclusive to the VBS phase space which can be seen in Tab. 9 by comparing the number of events in the different phase spaces. This is also what we have already seen in Fig. 26.

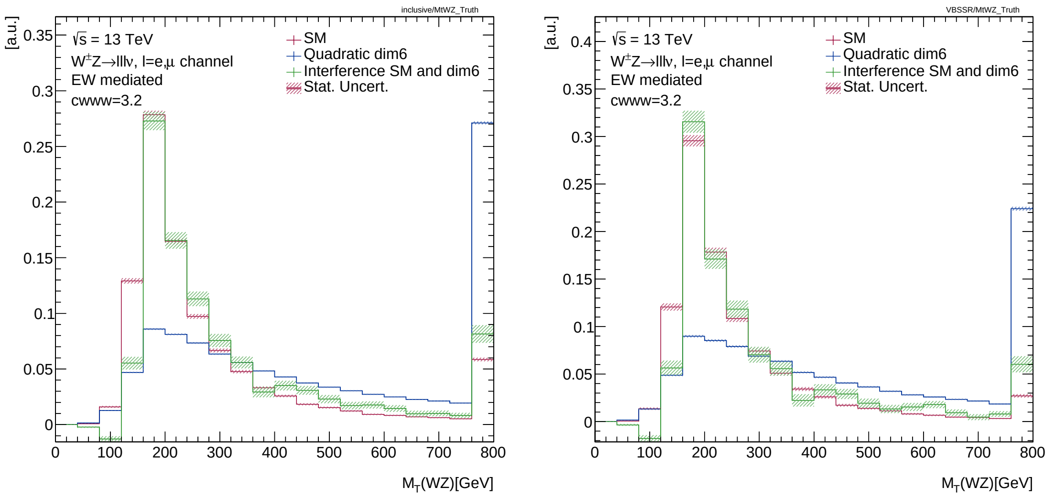

Figure 29 – The impact of the SM, interference part of the SM and the dimension six EFTs operator $\mathcal{O}_w$ and the quadratic part of the dimension six EFTs operator $\mathcal{O}_{www}$ with $cw = 3.2$ normalised to there number of events in the inclusive phase space (left) and in the VBS phase space (right) for EW mediated $W^\pm Z$ production and fully leptonic decay.

In Fig. 29, the shape of the interference of the SM and a dimension six EFTs operator and the quadratic effect of the dimension six EFTs operator with $\mathcal{O}_{www}$ as an example are shown in the inclusive phase space (left) and in the VBS phase space (right). The shape of the SM is also applied as a reference. The shape of interference and quadratic part completely do not change from one to the other phase space. The interference starts with a small positive impact but changes its sign shortly after $M_T^{W^\pm Z} = 100\,GeV$. Most of its impact ($\sim 75\%$) can be found in the region $100\,GeV < M_T^{W^\pm Z} < 350\,GeV$ with the maximum at $M_T^{W^\pm Z} = 200\,GeV$. For $M_T^{W^\pm Z} > 350\,GeV$ the distribution drops flat but still stays negative. The impact for the quadratic effect of dimension six EFTs operators increases from the the beginning to $M_T^{W^\pm Z} = 200\,GeV$, where it reaches its maximum. Directly from that point on, the distribution drops flat. Furthermore, the amount of events does not change for the interference between the standard model and a dimension six

EFTs operator and the quadratic part of a dimension six EFTs operator relative to the number of events that are given by the SM.

5.3 Dimension six operators in the inclusive phase space and VBS phase space

To study the impact of dimension six EFTs operators in the inclusive phase space the binning for the calculation of their limits is used (2.30). Since this binning is optimized for the impact dimension six EFTs operators of M_T^{VV} in the inclusive phase space and should give the largest impact it is reasonable to use them and we assume also the largest impact of dimension six EFTs operators in the VBS phase space. In the different bins first the number of events N are determined. The uncertainty of N is given by

$$\Delta N = \sqrt{N} \tag{5.2}$$

However the amount of the simulated events of the $W^{\pm}Z$ production is much lager than the assumed number of events given by integrated luminosity L_{int}. Therefore the generated number of events are scaled down to the finally used number of events are. The uncertainty ΔN is calculated on the amount of generated events with 5.2 and also scaled down. That procedure reduces the uncertainty of the used number of events.

With the number of events the ratio r between the SM with additional dimension six parameters and the SM itself can be calculated with 5.3. While the uncertainty Δr of r is determined with 5.4. Therefor the separated simulation of the SM the interference of the SM and the dimension six EFTs operators and the quadratic effect of the dimension six EFTs operators are exploited. Since theses samples are simulated separately for there own they are completely independent from each other and no covariance is need to be calculated. The ratio r shows the amount of events of dimension six EFTs operators normalized to the events that are given by the SM and can point up how significant the impact of dimension six EFTs operators is with regard to the impact of the SM.

$$\text{ratio} \equiv \frac{N_{SM+dim6}}{N_{SM}} = \frac{N_{SM} + N_{interf} + N_{quad}}{N_{SM}} = 1 + \frac{N_{interf} + N_{quad}}{N_{SM}} \tag{5.3}$$

$$\Delta r = \sqrt{\left(\frac{\partial r}{\partial N_{SM}}\Delta N_{SM}\right)^2 + \left(\frac{\partial r}{\partial N_{interf}}\Delta N_{interf}\right)^2 + \left(\frac{\partial r}{\partial N_{quad}}\Delta N_{quad}\right)^2} \tag{5.4}$$

$$= \sqrt{\left(-\frac{N_{interf} + N_{quad}}{N_{SM}^2}\Delta N_{SM}\right)^2 + \left(\frac{\Delta N_{interf}}{N_{SM}}\right)^2 + \left(\frac{\Delta N_{quad}}{N_{SM}}\right)^2} \tag{5.5}$$

Also the cross section σ is determined. Once for the SM (5.6) and also for the dimension six impact (5.8). Since we just have a look on simulated events the integrated luminosity L_{int} is assumed to be free of uncertainties. So the uncertainties $\Delta\sigma_{SM}$ and $\Delta\sigma_{dim6}$ are calculated with the propagation of uncertainties with 5.7 and 5.10. The cross section shows the impact of the SM and also the impact of the dimension six EFTs operators but unlike the ratio r independent from the SM.

$$\sigma_{SM} = \frac{N_{SM}}{L_{int}} \tag{5.6}$$

$$\Delta\sigma_{SM} = \frac{\partial \sigma}{\partial N_{SM}}\Delta N_{SM} = \frac{\Delta N_{SM}}{L_{int}} \tag{5.7}$$

$$\sigma_{dim6} = \frac{N_{dim6}}{L_{int}} = \frac{N_{interf} + N_{quad}}{L_{int}} \tag{5.8}$$

$$\Delta\sigma = \sqrt{\left(\frac{\partial \sigma}{\partial N_{interf}}\Delta N_{interf}\right)^2 + \left(\frac{\partial \sigma}{\partial N_{quad}}\Delta N_{quad}\right)^2} \tag{5.9}$$

$$= \sqrt{\left(\frac{\Delta N_{interf}}{L_{int}}\right)^2 + \left(\frac{\Delta N_{quad}}{L_{int}}\right)^2} \tag{5.10}$$

With the number of events N, the ratio r and the cross section σ we studied the dimension six EFTs operators in the inclusive phase space and in the VBS phase space to find out how much of the impact of the inclusive phase space is left in the VBS phase space and therefor the influence of dimension six parameters to limits of dimension eight operators in the VBS phase space.

5.3.1 Impact of dimension six EFTs operators in the inclusive phase space

QCD mediated $W^{\pm}Z$ production

The impact of the dimension six EFTs operator $\mathcal{O}_w$ with the channel dependent limits of the $W^{\pm}Z$ production for c_w/Λ^2 (Tab. 8) and the binning 2.30 for QCD mediated $W^{\pm}Z$ production in the inclusive phase space are shown in Fig. 30. In Tab. 10 the number of events N the ratio r and the cross section σ with there statistical uncertainties are given for each bin. It is visible that just the last two bins give a significant impact. Therefore this region of $M_T^{W^{\pm}}$ is used to calculate in general the value for the parameters c_i/Λ^2. But since we discussed the shapes of the interference of SM and dimension six EFTs operators and the quadratic part of dimension six EFTs operators in section 5.2.1, the sign flip of the interference at $M_T^{W^{\pm}} = 200\,GeV$ is also recognizable from bin $[140 - 180]\ GeV$ to $[180 - 250]\ GeV$. There the ratio r is getting greater than one. Furthermore in bin $[450 - 600]\ GeV$ the quadratic part of dimension six EFTs operators starts to be the dominating part. The reason for this is that for $c_w = -3.6$ the interference part has a negative impact in these region but r even though is greater one. This means that limits for the dimension six effects just can be calculated when the quadratic effect of dimension six EFTs operators dominates the impact. The impact of dimension six EFTs operators in the second last bin reaches up to $\sim 53\%$ of the cross section σ of the SM, while the impact reaches up to $\sim 195\%$ in the last bin.

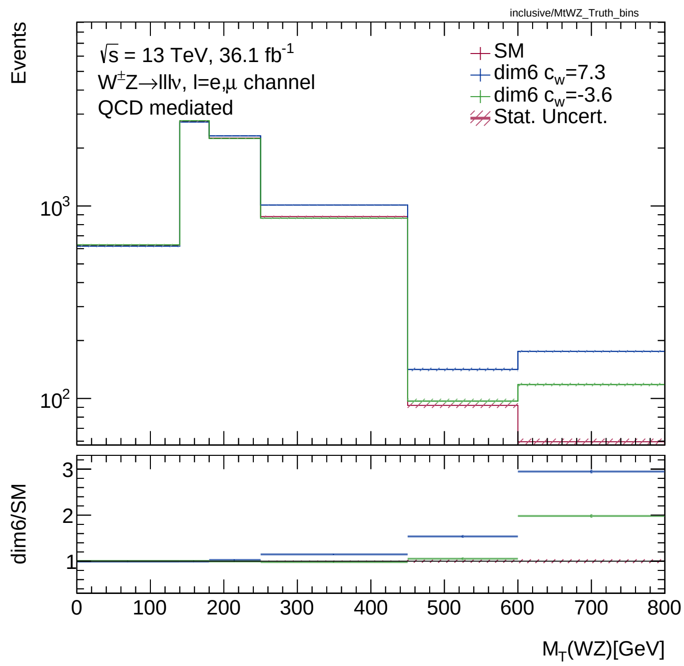

Figure 30 – The impact of the dimension six EFTs operator $\mathcal{O}_w$ for $M_T^{W^\pm Z}$ in the inclusive phase space for QCD mediated $W^\pm Z$ production and fully leptonic decay.

		$M_T^{W^\pm Z}$ $[GeV]$		
	couplings	[0 – 140]	[140 – 180]	[180 – 250]
events $[N]$	SM	624± 7	2753± 14	2253± 13
	$c_w = 7.3$	618± 7	2729± 14	2313± 13
	$c_w = -3.6$	628± 7	2771± 14	2242± 13
ratio r	$c_w = 7.3$	0.9910± 0.0005	0.99128± 0.00026	1.0266± 0.0004
	$c_w = -3.6$	1.00641± 0.00026	1.0654± 0.00013	0.99512± 0.00019
σ $[fb]$	SM	17.28± 0.19	76.3± 0.4	62.4± 0.4
	$c_w = 7.3$	-0.156± 0.009	-0.643± 0.020	1.658± 0.023
	$c_w = -3.6$	0.110 ±0.005	0.506± 0.010	-0.314± 0.012

		$M_T^{W^\pm Z}$ $[GeV]$		
	couplings	[250 – 450]	[450 – 600]	[600 – ∞]
events $[N]$	SM	881± 8	92± 3	60± 2
	$c_w = 7.3$	1011± 8	142 ±3	176± 2
	$c_w = -3.6$	864± 8	97± 3	118± 2
ratio r	$c_w = 7.3$	1.1473± 0.0017	1.537± 0.017	2.95± 0.08
	$c_w = -3.6$	0.9806± 0.0006	1.0529± 0.0033	1.982± 0.038
σ $[fb]$	SM	24.41± 0.23	2.550± 0.076	1.65± 0.07
	$c_w = 7.3$	3.608± 0.025	1.370± 0.014	3.214± 0.018
	$c_w = -3.6$	-0.474± 0.013	0.135± 0.008	1.621± 0.011

Table 10 – Number of events for the SM and SM with the dimension six EFTs operator $\mathcal{O}_w$, the ratio between the SM with the dimension six EFTs operator and the SM and σ for the SM and the impact of the dimension six EFTs operator for the QCD mediated $W^\pm Z$ production in the inclusive phase space.

EW mediated $W^{\pm}Z$ production

The impact of the dimension six EFTs operator $\mathcal{O}_{www}$ with the channel dependent limits of the $W^{\pm}Z$ production for c_{www}/Λ^2 (Tab. 8) and the binning 2.30 for EW mediated $W^{\pm}Z$ production in the inclusive phase space are shown in Fig. 31. In Tab. 11 the number of events N the ratio r and the cross section σ with there statistical uncertainties are given for each bin. Compared to the impact of the QCD mediated $W^{\pm}$ production the impact of EW mediated $W^{\pm}Z$ production is roughly five times smaller. And also effect of dimension six EFTs operators of EW mediated $W^{\pm}Z$ production accounts two percent of the QCD mediated $W^{\pm}Z$ effect. Therefore the impact of dimension six EFTs operators by a EW mediated $W^{\pm}Z$ production is negligible in the inclusive phase space. This agrees with the already used definition for the EW mediated $W^{\pm}Z$ production as background for the QCD mediated $W^{\pm}Z$ production in the inclusive phase space.

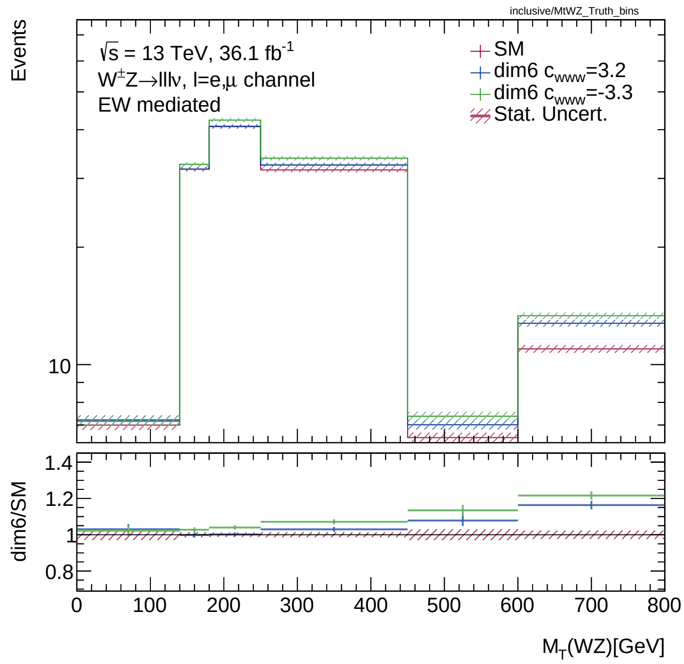

Figure 31 – The impact of the dimension six EFTs operator $\mathcal{O}_{www}$ for $M_T^{W^{\pm}Z}$ in the inclusive phase space for EW mediated $W^{\pm}Z$ production and fully leptonic decay.

		$M_T^{W^\pm Z}$ $[GeV]$		
	couplings	$[0-140]$	$[140-180]$	$[180-250]$
events $[N]$	SM	7± 1	32± 1	41± 1
	$c_{www}=3.2$	7± 1	32± 1	41± 1
	$c_{www}=-3.3$	7± 1	33± 1	42± 1
ratio r	$c_{www}=3.2$	1.0300± 0.0017	0.9987± 0.0006	1.0020± 0.0006
	$c_{www}=-3.3$	1.0214± 0.0016	1.0274± 0.0008	1.0398± 0.0008
σ $[fb]$	SM	0.194± 0.006	0.889± 0.012	1.128± 0.014
	$c_{www}=3.2$	0.00582± 0.00028	-0.0011± 0.0006	0.0019± 0.0007
	$c_{www}=-3.3$	0.00416± 0.00028	0.0241± 0.0006	0.0446± 0.0007

		$M_T^{W^\pm Z}$ $[GeV]$		
	couplings	$[250-450]$	$[450-600]$	$[600-\infty]$
events $[N]$	SM	32± 1	7± 1	11± 1
	$c_{www}=3.2$	32± 1	7± 1	13± 1
	$c_{www}=-3.3$	34± 1	7± 1	13± 1
ratio r	$c_{www}=3.2$	1.0295± 0.0011	1.078± 0.005	1.163± 0.005
	$c_{www}=-3.3$	1.0713± 0.0014	1.134± 0.006	1.216± 0.006
σ $[fb]$	SM	0.874± 0.012	0.180± 0.006	0.304± 0.007
	$c_{www}=3.2$	0.02576± 0.00088	0.0141± 0.0007	0.0498± 0.0007
	$c_{www}=-3.3$	0.06233± 0.00088	0.0244± 0.0007	0.0657± 0.0007

Table 11 – Number of events for the SM and SM with the dimension six EFTs operator $\mathcal{O}_{www}$, the ratio between the SM with the dimension six EFTs operator and the SM and σ for the SM and the impact of the dimension six EFTs operator for the EW mediated $W^\pm Z$ production in the inclusive phase space.

5.3.2 Impact of dimension operators in the VBS phase space

QCD mediated $W^\pm Z$ production

The impact of the dimension six EFTs operator $\mathcal{O}_w$ with the channel dependent limits of the $W^\pm Z$ production for c_w/Λ^2 (Tab. 8) and the binning 2.30 for QCD mediated $W^\pm Z$ production in the VBS phase space are shown in Fig. 32. In Tab. 12 the number of events N the ratio r and the cross section σ with there statistical uncertainties are given for each bin. The impact of dimension six EFTs operators for almost every bin is negligible with respect to the statistical uncertainties. Just the last bin gives an impact of $\sigma \approx 0.05\,fb$. A impact of dimension six EFTs operators of $\sim 28\%$ is given. So in the VBS phase space the QCD mediated $W^\pm Z$ processes and also the impact of dimension six EFTs operators for this process decrease distinctly.

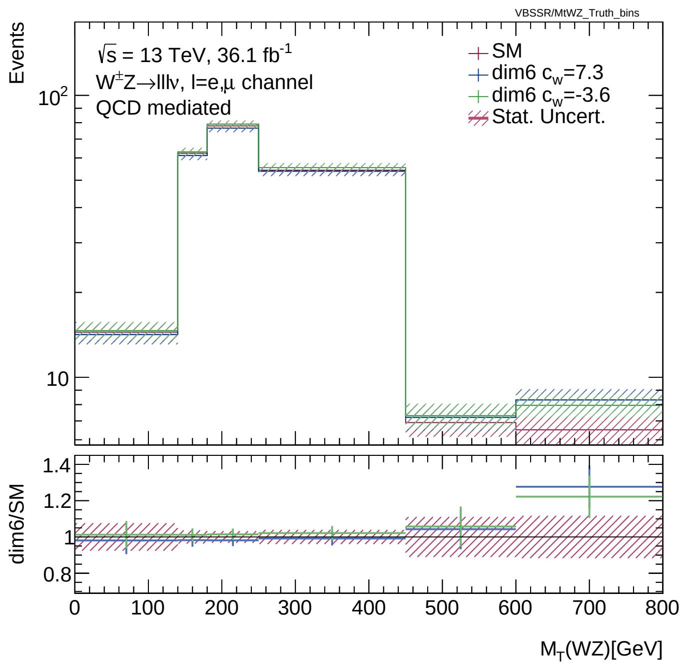

Figure 32 – The impact of the dimension six EFTs operator $\mathcal{O}_w$ for $M_T^{W^{\pm}Z}$ in the VBS phase space for QCD mediated $W^{\pm}Z$ production and fully leptonic decay.

		$M_T^{W^{\pm}Z}$ $[GeV]$		
	couplings	$[0-140]$	$[140-180]$	$[180-250]$
events $[N]$	SM	14± 1	62± 2	78± 2
	$c_w = 7.3$	14± 1	61± 1	77± 2
	$c_w = -3.6$	15± 1	63± 1	79± 2
ratio r	$c_w = 7.3$	0.9806± 0.0038	0.9823± 0.0018	0.9814± 0.0017
	$c_w = -3.6$	1.0124± 0.0017	1.0114± 0.0010	1.01424± 0.0010
σ $[fb]$	SM	0.401± 0.031	1.73± 0.06	2.16± 0.07
	$c_w = 7.3$	-0.0078± 0.0014	-0.0308± 0.0028	-0.00399± 0.0034
	$c_w = -3.6$	0.00499± 0.00056	0.020± 0.002	0.0307± 0.017

		$M_T^{W^{\pm}Z}$ $[GeV]$		
	couplings	$[250-450]$	$[450-600]$	$[600-\infty]$
events $[N]$	SM	54± 2	7± 1	7± 1
	$c_w = 7.3$	54± 1	7± 1	8± 1
	$c_w = -3.6$	55± 1	7± 1	8± 1
ratio r	$c_w = 7.3$	0.9917± 0.0029	1.043± 0.015	1.28± 0.04
	$c_w = -3.6$	1.0216± 0.0018	1.0579± 0.0010	1.223± 0.029
σ $[fb]$	SM	1.50± 0.06	0.191± 0.022	0.180± 0.021
	$c_w = 7.3$	-0.012± 0.005	0.0083± 0.0026	0.0499± 0.0031
	$c_w = -3.6$	0.0321± 0.0023	0.0111± 0.0013	0.0399± 0.0020

Table 12 – Number of events for the SM and SM with the dimension six EFTs operator $\mathcal{O}_w$, the ratio between the SM with the dimension six EFTs operator and the SM and σ for the SM and the impact of the dimension six EFTs operator for the QCD mediated $W^{\pm}Z$ production in the VBS phase space.

5.3.3 EW mediated $W^{\pm}Z$ production

EW mediated $W^{\pm}Z$ production

The impact of the dimension six EFTs operator $\mathcal{O}_{www}$ with the channel dependent limits of the $W^{\pm}Z$ production for c_{www}/Λ^2 (Tab. 8) and the binning 2.30 for EW mediated $W^{\pm}Z$ production in the VBS phase space are shown in Fig. 31. In Tab. 13 the number of events N the ratio r and the cross section σ with there statistical uncertainties are given for each bin. Only in the last two bins a impact of dimension six EFTs operators cab be found with the respect to the statistical uncertainties. The impact of dimension six EFTs operators reaches $\sim 15\%$ of the SM and in the last bin $\sim 33\%$. While the impact of the SM EW mediated $W^{\pm}Z$ production decreases to $\sim 20\%$ in the VBS phace space compared to the inclusive phase space.

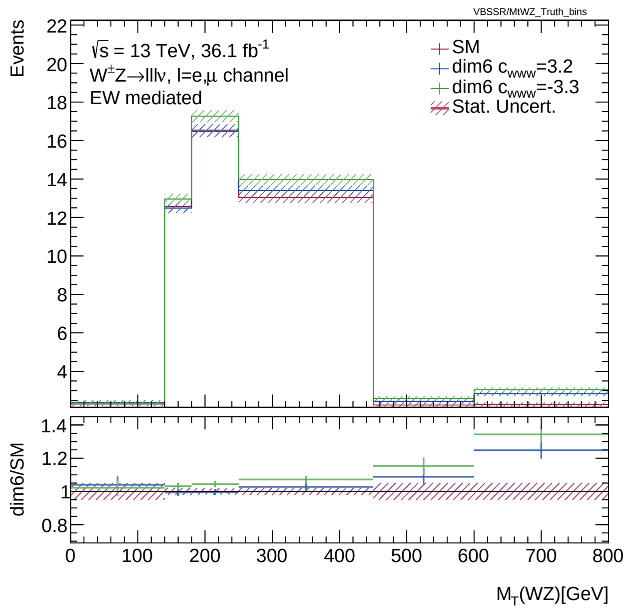

Figure 33 – The impact for the dimension six EFTs operator $\mathcal{O}_{www}$ with $c_{www} = 3.2$ and $c_{www} = -3.3$ of the transverse momentum of $W^{\pm}$ in the inclusive phase space (left) and in the VBS phase space (right) for EW mediated $W^{\pm}Z$ production and fully leptonic decay in the optimized binning for limit setting.

		$M_T^{W^\pm Z}$ $[GeV]$		
	couplings	$[0-140]$	$[140-180]$	$[180-250]$
events $[N]$	SM	2± 1	13± 1	17±1
	$c_{www}=3.2$	2± 1	13± 1	16±1
	$c_{www}=-3.3$	2± 1	13± 1	17±1
ratio r	$c_{www}=3.2$	1.0391± 0.0049	0.9936± 0.0009	0.9964± 0.0007
	$c_{www}=-3.3$	1.0217± 0.0045	1.0310± 0.0011	1.0435± 0.0015
σ $[fb]$	SM	0.0637± 0.0034	0.348± 0.008	0.458± 0.09
	$c_{www}=3.2$	0.00249± 0.00028	-0.00194± 0.00028	-0.00194± 0.00028
	$c_{www}=-3.3$	0.00139± 0.00028	0.01111± 0.00028	0.0199± 0.0006

		$M_T^{W^\pm Z}$ $[GeV]$		
	couplings	$[250-450]$	$[450-600]$	$[600-\infty]$
events $[N]$	SM	13± 1	2± 1	2± 1
	$c_{www}=3.2$	13± 1	2± 1	3± 1
	$c_{www}=-3.3$	14± 1	3± 1	3± 1
ratio r	$c_{www}=3.2$	1.0276± 0.0017	1.089± 0.007	1.247± 0.013
	$c_{www}=-3.3$	1.0721± 0.0022	1.156± 0.009	1.344± 0.018
σ $[fb]$	SM	0.361± 0.008	0.062± 0.003	0.0628± 0.0031
	$c_{www}=3.2$	0.0097± 0.0006	0.00554± 0.00028	0.01551± 0.00028
	$c_{www}=-3.3$	0.0258± 0.0006	0.00942± 0.00028	0.02161± 0.00028

Table 13 – The impact of the dimension six EFTs operator $\mathcal{O}_{www}$ for $M_T^{W^\pm Z}$ in the VBS phase space for EW mediated $W^\pm Z$ production and fully leptonic decay

Chapter 6

Conclusion

The simulation of the separated SM, interference and quadratic part fits well to the fully generated $W^{\pm}Z$ production. Using the separation of effects works fine for QCD and EW mediated $W^{\pm}Z$ production in the inclusive phase space and also in the VBS phase space. Also the scaling to different values of the dimension six parameters c_i/Λ^2 shows good result.
The assumption that $M_T^{W^{\pm}Z}$ is the most sensitive observable for the studies of the impact of dimension six EFTs operators confirms in the inclusive and also in the VBS phase space. To study the impact of dimension six EFTs operators in the VBS phase space the distribution of $M_T^{W^{\pm}Z}$ is also the best choice.
By studying the shape of the interference and quadratic effects of the dimension six EFTs operators it has been shown that the quadratic part dominates if the impact of dimension six EFTs operators has a significant impact. These occurs for the QCD and EW mediated $W^{\pm}Z$ production in the inclusive and VBS phase space.
The most sensitive range of $M_T^{W^{\pm}Z}$ for additional dimension six EFTs operators is given with $M_T^{W^{\pm}Z} > 600\,GeV$. In these range the cross section σ increases up to $\sim 195\%$ of the SM for the QCD mediated $W^{\pm}Z$ production in the inclusive phase space. So an impact of $(3.214 \pm 0.0018)\ fb$ occurs. In the VBS phase space the QCD mediated $W^{\pm}Z$ production decreases strongly and with it also the effect of dimension six EFTs operators to a maximum of $\sim 28\%$ compared to the SM. The cross section for the SM amounts to $\sigma = (0.180 \pm 0.021)\ fb$ and therefore the effect of dimension six EFTs operators is $\sigma = (0.0499 \pm 0.0031)\ fb$. So using VBS criteria reduces the impact in the $M_T^{W^{\pm}Z}$ distribution in the range $> 600\,GeV$ of dimension six EFTs operators by QCD mediated $W^{\pm}Z$ production to not even 2% of its effect in the inclusive phase space.
The impact of dimension six EFTs operators of the EW mediated $W^{\pm}Z$ production supplies not even 2% to the impact of the QCD mediated production in the range

of $M_T^{W^\pm Z} > 600\,GeV$. Therefore just the SM of these production can be defined as background for extraction of limits for dimension six EFTs operators by QCD mediated $W^\pm Z$ production. This agrees with to the already used procedure of dimension six limits extraction. The impact to $M_T^{W^\pm Z} > 600\,GeV$ for the SM EW mediated $W^\pm Z$ production decreases to $\sim 20\%$ with $\sigma = (0.0628 \pm 0.0031)\ fb$ in the VBS phase space. And the effect of dimension six EFTs operators with $\sigma = (0.02161 \pm 0.00028)\ fb$ halves itself.
Finally the QCD and EW mediated $W^\pm Z$ production have the same order of magnitude in the VBS phase space. The cross section in the range $M_T^{W^\pm Z} > 600\,GeV$, where the highest impact of dimension six EFTs operators is given, for the SM and dimension six EFTs operators are calculated with

QCD mediated $W^\pm Z$ production:

$$\begin{aligned}
\sigma_{tot}^{QCD} =& \sigma_{SM}^{QCD} + \sigma_{dim6}^{QCD} \\
=& (0.2299 \pm 0.0241)_{tot}\ fb \\
=& (0.180 \pm 0.021)_{SM}\ fb + (0.0499 \pm 0.0031)_{dim6}\ fb
\end{aligned}$$

EW mediated $W^\pm Z$ production:

$$\begin{aligned}
\sigma_{tot}^{EW} =& \sigma_{SM}^{EW} + \sigma_{dim6}^{EW} \\
=& (0.08 \pm 0.02)_{tot}\ fb \\
=& (0.0628 \pm 0.0031)_{SM}\ fb + (0.02161 \pm 0.00028)_{dim6}\ fb
\end{aligned}$$

Therefore dimension six EFTs operators have an impact of $\sim 30\%$ to the SM QCD and EW mediated $W^\pm Z$ production in the VBS phase space and should not be neglected in favor of dimension eight operators.

```
define p = g u c d s u~ c~ d~ s~ b b~
define j = g u c d s u~ c~ d~ s~ b b~
define l = e+ e- ve ve~
define v = mu+ mu- vm vm~
define W = W+ W-

#defined prosses for QCD mediated WZ production

generate p p > W Z > lllv NP^2==2 @0
add process p p > W Z > lllv j NP^2==2 @1
add process p p > W Z > lllv j j NP^2==2 @2

#defined prosses for EW mediated WZ production

generate p p > W Z > lllvjj QCD=0 NP^2==2 @0

#value of NP:
# NP==0 SM
# NP^2==2 interference
# NP==2 quadratic
# NP<=2 full
```

Figure 34 – Process definition for the simulated QCD and EW mediated $W^{\pm}Z$ production in MadGraph

```
###################################################################
## PARAM_CARD AUTOMATICALY GENERATED BY THE UFO  #####################
###################################################################

###################################
## INFORMATION FOR SMINPUTS
###################################
Block SMINPUTS
    1 1.279000e+02 # aEWM1
    2 1.166370e-05 # Gf
    3 1.184000e-01 # aS

###################################
## INFORMATION FOR MASS
###################################
Block MASS
    4 0.000000e+00 # MC
    5 0.000000e+00 # MB
    6 1.720000e+02 # MT
   13 0.000000e+00 # MM
   15 0.000000e+00 # MTA
   23 9.118760e+01 # MZ
   25 1.250000e+02 # MH
  9000006 1.250000e+02 # MP
##  Not dependent paramater.
## Those values should be edited following analytical the
## analytical expression. Some generator could simply ignore
## those values and use the analytical expression
  22 0.000000 # a : 0.0
  24 79.824360 # W+ : cmath.sqrt(MZ**2/2. + cmath.sqrt(MZ**4/4. - (aEW*cmath.pi*MZ**2)/(Gf*cmath.sqrt(2))))
  21 0.000000 # g : 0.0
  9000001 0.000000 # ghA : 0.0
  9000003 79.824360 # ghWp : cmath.sqrt(MZ**2/2. + cmath.sqrt(MZ**4/4. - (aEW*cmath.pi*MZ**2)/(Gf*cmath.sqrt(2))))
  9000004 79.824360 # ghWm : cmath.sqrt(MZ**2/2. + cmath.sqrt(MZ**4/4. - (aEW*cmath.pi*MZ**2)/(Gf*cmath.sqrt(2))))
  9000005 0.000000 # ghG : 0.0
  12 0.000000 # ve : 0.0
  14 0.000000 # vm : 0.0
  16 0.000000 # vt : 0.0
  2 0.000000 # u : 0.0
  1 0.000000 # d : 0.0
  3 0.000000 # s : 0.0
  251 79.824360 # G+ : cmath.sqrt(MZ**2/2. + cmath.sqrt(MZ**4/4. - (aEW*cmath.pi*MZ**2)/(Gf*cmath.sqrt(2))))
  11 0.000000 # e- : 0.0
###################################
## INFORMATION FOR DECAY
###################################
DECAY   6 1.508336e+00
DECAY  15 0.000000e-12
DECAY  23 2.495200e+00
DECAY  24 2.085000e+00
DECAY  25 6.382339e-03
DECAY 9000006 6.382339e-03
##  Not dependent paramater.
## Those values should be edited following analytical the
## analytical expression. Some generator could simply ignore
## those values and use the analytical expression
DECAY  22 0.000000 # a : 0.0
DECAY  21 0.000000 # g : 0.0
DECAY  9000001 0.000000 # ghA : 0.0
DECAY  9000002 0.000000 # ghZ : 0.0
DECAY  9000003 0.000000 # ghWp : 0.0
DECAY  9000004 0.000000 # ghWm : 0.0
DECAY  9000005 0.000000 # ghG : 0.0
DECAY  12 0.000000 # ve : 0.0
DECAY  14 0.000000 # vm : 0.0
DECAY  16 0.000000 # vt : 0.0
DECAY  2 0.000000 # u : 0.0
DECAY  4 0.000000 # c : 0.0
DECAY  1 0.000000 # d : 0.0
DECAY  3 0.000000 # s : 0.0
DECAY  5 0.000000 # b : 0.0
DECAY  250 0.000000 # G0 : 0.0
DECAY  251 0.000000 # G+ : 0.0
DECAY  11 0.000000 # e- : 0.0
DECAY  13 0.000000 # mu- : 0.0
```

```
###################################
## INFORMATION FOR DIM6
###################################
Block DIM6
    1 scan1: [3.2,0.0,0.0] # CWWWL2
    2 scan1: [0.0,7.3.0,0.0] # CWL2
    3 scan1: [0.0,0.0,136.0] # CBL2
    4 0.000000e+00 # CPWWWL2
    5 0.000000e+00 # CPWL2
    6 0.000000e+00 # CphidL2
    7 0.000000e+00 # CphiWL2
    8 0.000000e+00 # CphiBL2

###################################
## INFORMATION FOR WOLFENSTEIN
###################################
Block Wolfenstein
    1 0.000000e+00 # lamWS
    2 0.000000e+00 # AWS
    3 0.000000e+00 # rhoWS
    4 0.000000e+00 # etaWS

###################################
## INFORMATION FOR YUKAWA
###################################
Block YUKAWA
    4 0.000000e+00 # ymc
    5 0.000000e+00 # ymb
    6 1.720000e+02 # ymt
   13 0.000000e+00 # ymm
   15 0.000000e+00 # ymtau
#===========================================================
# QUANTUM NUMBERS OF NEW STATE(S) (NON SM PDG CODE)
#===========================================================

Block QNUMBERS 9000001  # ghA
        1 0  # 3 times electric charge
        2 -1  # number of spin states (2S+1)
        3 1  # colour rep (1: singlet, 3: triplet, 8: octet)
        4 1  # Particle/Antiparticle distinction (0=own anti)
Block QNUMBERS 9000002  # ghZ
        1 0  # 3 times electric charge
        2 -1  # number of spin states (2S+1)
        3 1  # colour rep (1: singlet, 3: triplet, 8: octet)
        4 1  # Particle/Antiparticle distinction (0=own anti)
Block QNUMBERS 9000003  # ghWp
        1 3  # 3 times electric charge
        2 -1  # number of spin states (2S+1)
        3 1  # colour rep (1: singlet, 3: triplet, 8: octet)
        4 1  # Particle/Antiparticle distinction (0=own anti)
Block QNUMBERS 9000004  # ghWm
        1 -3  # 3 times electric charge
        2 -1  # number of spin states (2S+1)
        3 1  # colour rep (1: singlet, 3: triplet, 8: octet)
        4 1  # Particle/Antiparticle distinction (0=own anti)
Block QNUMBERS 9000005  # ghG
        1 0  # 3 times electric charge
        2 -1  # number of spin states (2S+1)
        3 8  # colour rep (1: singlet, 3: triplet, 8: octet)
        4 1  # Particle/Antiparticle distinction (0=own anti)
Block QNUMBERS 250  # G0
        1 0  # 3 times electric charge
        2 1  # number of spin states (2S+1)
        3 1  # colour rep (1: singlet, 3: triplet, 8: octet)
        4 0  # Particle/Antiparticle distinction (0=own anti)
Block QNUMBERS 251  # G+
        1 3  # 3 times electric charge
        2 1  # number of spin states (2S+1)
        3 1  # colour rep (1: singlet, 3: triplet, 8: octet)
        4 1  # Particle/Antiparticle distinction (0=own anti)
Block QNUMBERS 9000006  # h1
        1 0  # 3 times electric charge
        2 1  # number of spin states (2S+1)
        3 1  # colour rep (1: singlet, 3: triplet, 8: octet)
        4 0  # Particle/Antiparticle distinction (0=own anti)
```

Figure 35 – Parameter card for the simulated QCD and EW mediated $W^{\pm}Z$ production in MadGraph

Bibliography

[1] M. Aaboud et al. “Study of WW gamma and WZ gamma production in pp collisions at root s=8 TeV and search for anomalous quartic gauge couplings with the ATLAS experiment”. In: *European Physical Journal C* 77.9, 646 (2017). DOI: 10.1140/epjc/s10052-017-5180-3.

[2] G. Aad et al. “Observation of a new particle in the search for the Standard Model Higgs boson with the ATLAS detector at the LHC”. In: *Physics Letters B* 716.1 (2012), pp. 1–29. ISSN: 0370-2693. DOI: https://doi.org/10.1016/j.physletb.2012.08.020. URL: http://www.sciencedirect.com/science/article/pii/S037026931200857X.

[3] P Anger et al. *A Measurement of WZ Production in Proton-Proton Collisions at $\sqrt{\mathbf{s}} = \mathbf{8}$ TeV with the ATLAS Detector*. Tech. rep. ATL-COM-PHYS-2014-144. Geneva: CERN, Feb. 2014. URL: https://cds.cern.ch/record/1663539.

[4] Carsten Bittrich et al. *Study of electroweak $W^{\pm}Z$ boson pair production in association with two jets in pp collisions at $\sqrt{s} = 13$ TeV with the ATLAS Detector*. Tech. rep. ATL-COM-PHYS-2018-025. Geneva: CERN, Jan. 2018. URL: https://cds.cern.ch/record/2300058.

[5] W. Buchmueller and D. Wyler. “Effective lagrangian analysis of new interactions and flavour conservation”. In: *Nuclear Physics B* 268.3 (1986), pp. 621–653. ISSN: 0550-3213. DOI: https://doi.org/10.1016/0550-3213(86)90262-2. URL: http://www.sciencedirect.com/science/article/pii/0550321386902622.

[6] Celine Degrande. *Effective field theory for weak boson pair production*. https://cp3.irmp.ucl.ac.be/projects/madgraph/wiki/Models/EWdim6. Aug. 2019.

[7] Christian Theis,Winfried Kernbichler. *Grundlagen der Monte Carlo Methoden*. https://itp.tugraz.at/MML/MonteCarlo/MCIntro.pdf. May 2002.

[8] The ATLAS Collaboration. “The ATLAS Experiment at the CERN Large Hadron Collider”. In: *Journal of Instrumentation* 3.08 (2008), S08003. URL: http://stacks.iop.org/1748-0221/3/i=08/a=S08003.

[9] Celine Degrande et al. *Monte Carlo tools for studies of non-standard electroweak gauge boson interactions in multi-boson processes: A Snowmass White Paper*. 2013. eprint: arXiv:1309.7890.

[10] *Expected performance of the ATLAS experiment: detector, trigger and physics*. Geneva: CERN, 2009. URL: http://cds.cern.ch/record/1125884.

[11] Raquel Gomez-Ambrosio. “Studies of dimension-six EFT effects in vector boson scattering”. In: *The European Physical Journal C* 79.5 (May 2019), p. 389. ISSN: 1434-6052. DOI: 10.1140/epjc/s10052-019-6893-2. URL: https://doi.org/10.1140/epjc/s10052-019-6893-2.

[12] D. Griffiths. *Introduction to Elementary Particles*. Second, Revised Edition. New York, USA: John Wiley & Sons, 1987.

[13] B. Grzadkowski et al. “Dimension-six terms in the Standard Model Lagrangian”. In: *Journal of High Energy Physics* 2010.10 (Oct. 2010), p. 85. ISSN: 1029-8479. DOI: 10.1007/JHEP10(2010)085. URL: https://doi.org/10.1007/JHEP10(2010)085.

[14] Hannes Mildner. *MadGraphEFTMCdecomposition*. https://twiki.cern.ch/twiki/bin/viewauth/AtlasProtected/MadGraphEFTMCdecomposition. Nov. 2018.

[15] Brian Henning et al. “2, 84, 30, 993, 560, 15456, 11962, 261485, . . .: higher dimension operators in the SM EFT”. In: *Journal of High Energy Physics* 2017.8 (Aug. 2017), p. 16. ISSN: 1029-8479. DOI: 10.1007/JHEP08(2017)016. URL: https://doi.org/10.1007/JHEP08(2017)016.

[16] Johan Alwall. *Event Generation with MadGraph 5*. https://cp3.irmp.ucl.ac.be/projects/madgraph/raw-attachment/wiki/SchoolNTU/NTU-MG5-lectures.pdf. May 2012.

[17] David Landau and Kurt Binder. *A Guide to Monte Carlo Simulations in Statistical Physics*. New York, NY, USA: Cambridge University Press, 2005. ISBN: 0521842387.

[18] *Measurement of $W^{\pm}Z$ boson pair-production in pp collisions at $\sqrt{s} = 13$ TeV with the ATLAS Detector and confidence intervals for anomalous triple gauge boson couplings*. Tech. rep. ATLAS-CONF-2016-043. Geneva: CERN, Aug. 2016. URL: https://cds.cern.ch/record/2206093.

[19] Particle Data Grou. *W Boson*. http://pdg.lbl.gov/2019/listings/rpp2019-list-w-boson.pdf. 2018/19.

[20] Particle Data Grou. *Z Boson*. http://pdg.lbl.gov/2019/listings/rpp2019-list-z-boson.pdf. 2018/19.

[21] Schoeder Peskin. *An Introduction To Quantum Field Theory -*. New York: Avalon Publishing, 1995. ISBN: 978-0-813-34543-7.

[22] Povh Rith. *Teilchen und Kerne - Eine Einfuehrung in die physikalischen Konzepte*. 7th ed. Berlin Heidelberg New York: Springer-Verlag, 2013. ISBN: 978—3-6-42-97-4.

[23] Robert Rueger. *Monte Carlo Methodenin der statistischen Physikund ihre Anwendung zurSimulation von Spinsystemen*. http://work.robertrueger.de/docs/bscthesis.pdf. Sept. 2011.

[24] Reuven Y. Rubinstein and Dirk P. Kroese. *Simulation and the Monte Carlo Method*. 3rd. Wiley Publishing, 2016. ISBN: 1118632168, 9781118632161.

[25] *Search for anomalous couplings in semileptonic WW and WZ decays at sqrt(s) = 13 TeV*. Tech. rep. CMS-PAS-SMP-18-008. Geneva: CERN, 2019. URL: https://cds.cern.ch/record/2672271.

[26] University of Zurich, physics institute. *The standard model*. https://www.physik.uzh.ch/en/researcharea/lhcb/outreach/StandardModel.html/. July 2019.